Chapter 1
Single Neuron Modeling

In this introductory chapter we describe conductance-based models of single neurons, which take into account action potential generation, the effects of external stimuli, synaptic and dendritic processing, and ion channel fluctuations. In the appendix we provide an informal introduction to stochastic calculus. In Chap. 2 we turn to the classical theory of waves in one-dimensional neural media, as exemplified by action potential propagation along axons. This will introduce some of the techniques used throughout the book, including phase-plane analysis, slow–fast systems, stability theory and Evans functions, averaging theory, and stochastic wave propagation. We then consider two examples of intracellular waves propagating along spiny dendrites (Chap. 3): the spike–diffuse–spike model of calcium-mediated spikes and a reaction–diffusion model of CaMKII translocation waves. A number of additional methods will be presented, including the analysis of waves in spiking models, homogenization theory, and the theory of pulled fronts. Finally, in Chap. 4 we consider both intracellular and intercellular calcium waves, emphasizing aspects that are specific to neurons. In particular, we highlight the important role of calcium signaling in astrocytes.

1.1 Conductance-Based Model of a Neuron

Cortical neurons typically consist of a cell body (or soma) where the nucleus containing DNA is located, a branching output structure known as the *axon* and a branching input structure known as the *dendritic tree*; see Fig. 1.1. Neurons mainly communicate with each other by sending electrical impulses or spikes (action potentials) along their axons. (Some neurons are also coupled diffusively via gap junctions [126].) These axons make contacts on the dendrites of other neurons via microscopic junctions known as *synapses*. The arrival of an electrical spike at a synaptic junction leads to the flow of electrical current along the dendritic tree of the stimulated neuron. If the total synaptic current from all of the activated synapses forces the electrical potential within the cell body to cross some threshold, then the neuron

fires a spike. The standard biophysical model for describing the dynamics of a single neuron with somatic membrane potential v is based upon conservation of electric charge:

$$C\frac{dv}{dt} = -I_{\text{con}} + u + I_{\text{ext}}, \tag{1.1}$$

where C is the cell capacitance, I_{con} is the membrane current, u denotes the sum of synaptic currents entering the cell body, and I_{ext} describes any externally injected currents. Ions can diffuse in and out of the cell through ion specific channels embedded in the cell membrane. Ion pumps within the cell membrane maintain concentration gradients, such that there is a higher concentration of Na$^+$ and Ca^{2+} outside the cell and a higher concentration of K$^+$ inside the cell. The membrane current through a specific channel varies approximately linearly with changes in the potential v relative to some equilibrium or reversal potential, which is the potential at which there is a balance between the opposing effects of diffusion and electrical forces. Summing over all channel types, the total membrane current (flow of positive ions) leaving the cell through the cell membrane is

$$I_{\text{con}} = \sum_s g_s(v - V_s), \tag{1.2}$$

where g_s is the conductance due to channels of type s and V_s is the corresponding reversal potential. In the case of a channel selective to a single ion, V_s satisfies the Nernst equation

$$V_s = \frac{k_B T}{q} \ln\left(\frac{[outside]_s}{[inside]_s}\right), \tag{1.3}$$

where q is the charge of the ion, k_B is the Boltzmann constant, T is temperature (in degrees Kelvin), and $[outside]_s, [inside]_s$ denote the extracellular and intracellular concentrations of the given ion. Typical values for the common ion species are $V_K \approx -75\,\text{mV}$, $V_{\text{Na}} \approx 50\,\text{mV}$, $V_{\text{Ca}} \approx 150\,\text{mV}$, and $V_{\text{Cl}} \approx -60\,\text{mV}$ (which is close to the resting potential of the cell).

The generation and propagation of an action potential arises from nonlinearities associated with active membrane conductances. Recordings of the current flowing through single channels indicate that channels fluctuate rapidly between open and closed states in a stochastic fashion. Nevertheless, most models of a neuron use deterministic descriptions of conductance changes, under the assumption that there are a large number of approximately independent channels of each type. It then follows from the law of large numbers that the fraction of channels open at any given time is approximately equal to the probability that any one channel is in an open state. The conductance g_s for ion channels of type s is thus taken to be the product $g_s = \bar{g}_s P_s$ where $\bar{g}_s$ is equal to the density of channels in the membrane multiplied by the conductance of a single channel and P_s is the fraction of open channels. The voltage dependence of the probabilities P_s in the case of a delayed-rectifier K$^+$ current and a fast Na$^+$ current was originally obtained by Hodgkin and Huxley [279] as part of their Nobel Prize winning work on the generation of action potentials in the squid giant axon. The delayed-rectifier K$^+$ current is responsible for
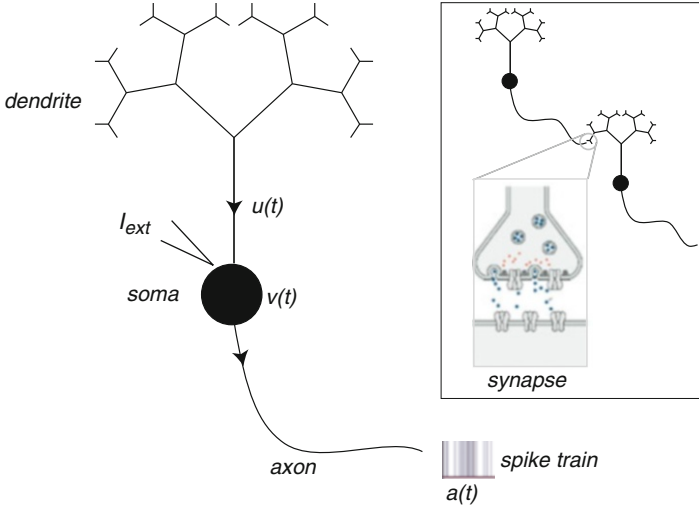
Fig. 1.1 Basic structure of a neuron. (Inset shows a synaptic connection from an upstream or presynaptic neuron and a downstream or postsynaptic neuron.) See text for details

terminating an action potential by repolarizing a neuron. One finds that opening of the K^+ channel requires structural changes in 4 identical and independent subunits so that $P_K = n^4$ where n is the probability that any one gate subunit has opened. In the case of the fast Na^+ current, which is responsible for the rapid depolarization of a cell leading to action potential generation, the probability of an open channel takes the form $P_{Na} = m^3 h$ where m^3 is the probability that an activating gate is open and h is the probability that an inactivating gate is open. Depolarization causes m to increase and h to decrease, whereas hyperpolarization has the opposite effect.

The dynamics of the gating variables m, n, h are usually formulated in terms of a simple kinetic scheme that describes voltage-dependent transitions of each gating subunit between open and closed states. More specifically, for each $X \in \{m, n, h\}$

$$\frac{dX}{dt} = \alpha_X(v)(1 - X) - \beta_X(v)X, \tag{1.4}$$

where $\alpha_X(v)$ is the rate of the transition *closed* $\rightarrow$ *open* and $\beta_X(v)$ is the rate of the reverse transition *open* $\rightarrow$ *closed*. Equation (1.4) can be rewritten in the alternative form

$$\tau_X(v)\frac{dX}{dt} = X_\infty(v) - X, \qquad \text{with } X \in \{m, n, h\}, \tag{1.5}$$

where

$$\tau_X(v) = \frac{1}{\alpha_X(v) + \beta_X(v)}, \qquad X_\infty(v) = \alpha_X(v)\tau_X(v).$$

It follows that the conductance variables m, n, and h approach the asymptotic values $m_\infty(v)$, $n_\infty(v)$, and $h_\infty(v)$ exponentially with time constants $\tau_m(v)$, $\tau_n(v)$, and $\tau_h(v)$,

respectively. From basic thermodynamic arguments, the opening and closing rates are expected to be exponential functions of the voltage. Hodgkin and Huxley [279] fitted exponential-like functions to the experimental data obtained from the squid axon:

$$\alpha_m = \frac{0.1(v+40)}{1-\exp[-0.1(v+40)]} \qquad \alpha_h = 0.07\exp[-0.05(v+65)],$$

$$\alpha_n = \frac{0.01(v+55)}{1-\exp[-0.1(v+55)]} \qquad \beta_m = 4.0\exp[-0.556(v+65)],$$

$$\beta_h = \frac{1}{1+\exp[-0.1(v+35)]} \qquad \beta_n = 0.125\exp[-0.125(v+65)].$$

All potentials are measured in mV, all times in ms, and all currents in $\mu A/cm^2$. The corresponding asymptotic functions $X_\infty(v)$ and time constants $\tau_X(v)$ are plotted in Fig. 1.2.
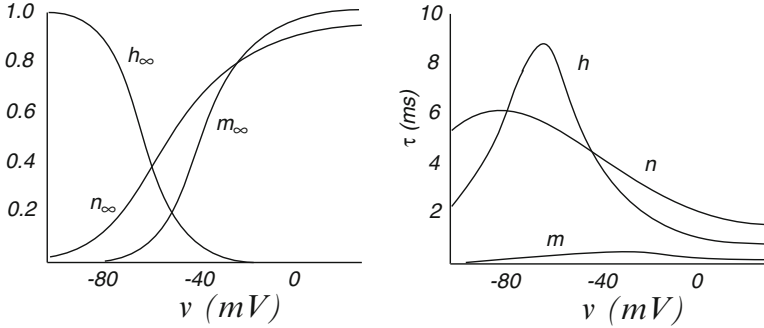
Fig. 1.2 Voltage-dependent steady-state levels of activation and inactivation (*left panel*) and voltage-dependent time constants (*right panel*) for the Hodgkin–Huxley model

We can now write down the Hodgkin–Huxley model for the generation of an action potential, which takes the membrane current to be the sum of a leakage current, a delayed-rectifier K$^+$ current, and a fast Na$^+$ current,

$$C\frac{dv}{dt} = f(v,m,n,h) + I_{\text{ext}}, \tag{1.6}$$

with

$$f(v,m,n,h) = -\bar{g}_{\text{Na}}m^3h(v-V_{\text{Na}}) - \bar{g}_{\text{K}}n^4(v-V_{\text{K}}) - \bar{g}_{\text{L}}(v-V_{\text{L}}). \tag{1.7}$$

The maximal conductances and reversal potentials used in the original model are $\bar{g}_{\text{L}} = 0.003\,\text{ms/mm}^2$, $\bar{g}_{\text{K}} = 0.36\,\text{mS/mm}^2$, $\bar{g}_{\text{Na}} = 1.2\,\text{mS/mm}^2$, $V_{\text{L}} = -54.387\,\text{mV}$, $V_{\text{K}} = -77\,\text{mV}$, and $V_{\text{Na}} = 50\,\text{mV}$. Note that the leakage current groups together various voltage-independent processes such as the currents carried by ion pumps that maintain the concentration gradients. The variables m,n,h evolve according to (1.4). The temporal evolution of the variables v, f, m, n, h during a single action potential is

shown in Fig. 1.3. Injection of a depolarizing current induces a rapid increase in the *m* variable describing activation of the Na$^+$ current. Since the slower *h* variable is initially around 0.6, there is a large influx of Na$^+$ ions, producing a sharp downward spike in the membrane current and a rapid depolarization through positive feedback. However, the rise in the membrane potential causes the Na$^+$ conductance to inactivate by driving *h* towards zero. In addition, the depolarization activates the K$^+$ conductance, resulting in a subsequent hyperpolarization.
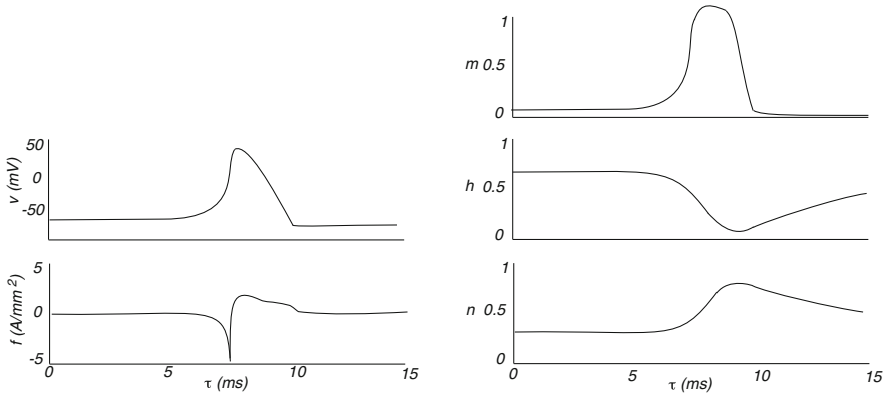
Fig. 1.3 The dynamics of v, f, n, m, h in the Hodgkin–Huxley model during the firing of an action potential induced by a current injection at $t = 5$ ms

Once a neuron has generated an action potential, it propagates as a traveling pulse along the axon of the neuron. In order to model a propagating action potential, it is necessary to combine the Hodgkin–Huxley conductance-based model given by (1.4) and (1.6) with a one-dimensional cable equation describing passive voltage changes along an axon or dendrite. The result is a partial differential equation of the form

$$C\frac{\partial v}{\partial t} = K\frac{\partial^2 v}{\partial x^2} + f(v, m, n, h), \tag{1.8}$$

where K is related to the membrane space constant of the cable; see Sect. 1.4, and $X = m, n, h$ evolve according to (1.4). Equation (1.8) is an example of a nonlinear reaction–diffusion equation used to model wave propagation in an excitable medium; one characteristic of an excitable medium is that it cannot support the passing of another wave until a certain amount of time has passed (known as the refractory period). A rigorous proof of the existence of traveling wave solutions of the spatially extended Hodgkin–Huxley equations has been developed [104, 267]. However, following standard treatments of waves in excitable media [242, 322, 444], we will develop the theory by considering the simpler FitzHugh–Nagumo model [192, 446]; see Chap. 2.

There is an ongoing debate about how best to characterize the output of a neuron, from either a dynamical systems or an information processing perspective. It is generally agreed that the detailed shape of an action potential is usually unimportant, so, at the fine temporal scale of a few milliseconds, the output of a neuron can be

represented in terms of the times at which the neuron fires an action potential (or spike). Given the conductance-based model (1.1), one typically identifies a firing threshold κ such that if $v(t)$ crosses the threshold from below at time $t = T$, then the neuron fires an action potential. If T^m denotes the mth firing time of the neuron since $t = 0$, say, then we have the threshold condition

$$T^m = \inf\{t, t > T^{m-1} | v(t) = \kappa, \dot{v}(t) > 0\}. \tag{1.9}$$

As an alternative to a spike timing representation of neuronal output, one can consider a rate-based representation that is obtained by filtering the spike train with some causal integral kernel $\Gamma(t)$, $\Gamma(t) = 0$ for $t < 0$:

$$z(t) = \sum_m \Gamma(t - T^m) = \int_{-\infty}^{\infty} \Gamma(t - \tau)a(\tau)d\tau, \tag{1.10}$$

where

$$a(t) = \sum_m \delta(t - T^m). \tag{1.11}$$

For example, if $\Gamma(t) = T^{-1}$ for $0 \le t < T$ and is zero otherwise, then $z(t)$ simply counts the number of spikes within the time interval $[t - T, t]$. In the special case of a regular spike train with $T^{m+1} - T^m = \Delta_0$ for all m, $z(t) = 1/\Delta_0$ in the limit $T \to \infty$.

Suppose, for the moment, that we ignore synaptic currents and consider what happens as the external input I_{ext} to a neuron is increased. Experimentally it is found that most cortical neurons switch from a resting state characterized by a low rate of (noise-driven) spontaneous firing to an active state characterized by either tonic (regular, repetitive) firing or bursting [131]. There has been considerable theoretical work on the transitions from resting to active states in conductance-based models based on bifurcation theory; see [173, 301] for excellent reviews. We will focus on tonic firing neurons, since these comprise the majority of cells in cortical networks. In the case of constant input $I_{ext} = I$, the firing rate $\bar{z}$ (mean number of spikes per second) of the neuron is typically found to be a nonlinear function of the input:

$$\bar{z} = F(I) \tag{1.12}$$

with the form of F depending on the nature of the bifurcation from the stable resting state to repetitive firing. A common bifurcation scenario in conductance-based models of cortical neurons is a saddle–node on an invariant circle [173, 301], which is classified as type I excitability. Close to the bifurcation point (see Fig. 1.4), we have

$$F(I) = F_0\sqrt{I - I_c}, \tag{1.13}$$

where I_c is the critical current for onset of regular spiking. (Another common form of excitability is type II, in which the loss of stability of the resting state and the transition to repetitive firing occur via a Hopf bifurcation. There are also more exotic

forms of excitability as detailed elsewhere [201, 423].) If one includes stochastic effects arising from synaptic and membrane noise, for example, then the effective mean firing rate becomes a smooth sigmoid-like function of injected current,

$$F(I) = \frac{F_0}{1 + e^{-\eta(I - \kappa)}}, \tag{1.14}$$

where η is the gain and κ is the firing threshold. In the high-gain limit $\eta \to \infty$, this reduces to a Heaviside firing rate function

$$F(I) = F_0 H(I - \kappa) = \begin{cases} F_0 & \text{if } I > \kappa \\ 0 & \text{if } I < \kappa. \end{cases} \tag{1.15}$$

Yet another commonly used firing rate function is the piecewise linear function

$$F(I) = \begin{cases} 0, & I < \kappa, \\ \eta(u - \kappa), & \kappa < I < \kappa + \eta^{-1}, \\ 1, & I > \kappa + \eta^{-1}. \end{cases} \tag{1.16}$$

This preserves the hard threshold of the saddle–node on a limit cycle bifurcation but ensures that the firing rate saturates at high input currents.
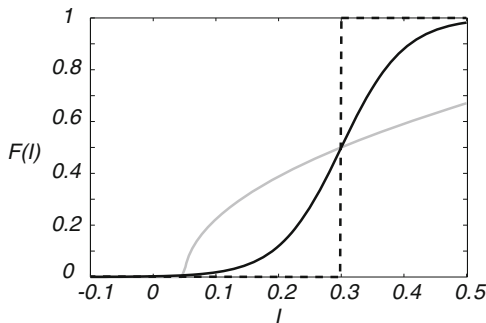
Fig. 1.4 Various forms of the nonlinear firing rate function $F(I)$. Sigmoid function (*black curve*) and Heaviside function (*dashed curve*) have a threshold $\kappa = 0.3$, whereas the square root function (*gray curve*) has a critical current $I_c = 0.05$

   The issue of how to represent a single neuron becomes even more salient when considering synaptically coupled spiking networks (Chap. 5) and neural fields (Chap. 6). In order to make analytical progress, it is necessary either to consider a very simple model of a spiking neuron such as integrate-and-fire [323] (Sect. 5.3) or to carry out some form of reduction of a conductance-based model. In the case of weakly coupled neural oscillators, one can reduce the dynamics to a network of coupled phase oscillators; see Chap. 5. The basic ideas underlying so-called phase reduction methods can be understood by considering the simpler case of a single, periodically forced neural oscillator.

1.2 Periodically Forced Neural Oscillator

A conductance-based model of a neuron with constant input current can be formulated as an M-dimensional ($M \geq 2$) system of ODEs

$$\frac{d\mathbf{x}}{dt} = \mathbf{f}(\mathbf{x}), \qquad \mathbf{x} = (x_1, \ldots x_M). \tag{1.17}$$

Here x_1, say, represents the membrane potential of the neuron (treated as a point processor) and x_m, $m > 1$, represent various ionic channel gating variables. Suppose that the neuron has a stable periodic solution $\mathbf{x}(t) = \mathbf{x}(t + \Delta_0)$ where $\omega_0 = 2\pi/\Delta_0$ is the *natural frequency* of the oscillator. In *phase space* the solution is an isolated attractive trajectory called a *limit cycle*. The dynamics on the limit cycle can be described by a uniformly rotating phase such that

$$\frac{d\theta}{dt} = \omega_0, \tag{1.18}$$

and $\mathbf{x}(t) = \mathbf{g}(\theta(t))$ with $\mathbf{g}$ a 2π-periodic function. Note that the phase is *neutrally stable* with respect to perturbations along the limit cycle—this reflects invariance of an autonomous dynamical system with respect to time shifts. Now suppose that a small external periodic input is applied to the oscillator such that

$$\frac{d\mathbf{x}}{dt} = \mathbf{f}(\mathbf{x}) + \varepsilon \mathbf{p}(\mathbf{x},t), \tag{1.19}$$

where $\mathbf{p}(\mathbf{x},t) = \mathbf{p}(\mathbf{x}, t + \Delta)$ and $\omega = 2\pi/\Delta$ is the forcing frequency. If the amplitude ε is sufficiently small and the cycle is stable, then deviations transverse to the limit cycle are small so that the main effect of the perturbation is to induce shifts in the phase. Therefore, we need to extend the definition of phase to a neighborhood of the limit cycle. This leads to the notion of an *isochrone* [221, 350, 679].

1.2.1 Isochrones and Phase-Resetting Curves

Suppose that we observe the unperturbed system stroboscopically at time intervals of length Δ_0. This leads to a Poincare mapping

$$\mathbf{x}(t) \to \mathbf{x}(t + \Delta_0) \equiv \mathscr{P}(\mathbf{x}(t)).$$

This mapping has all points on the limit cycle as fixed points. Choose a point $\mathbf{x}^*$ on the cycle and consider all points in the vicinity of $\mathbf{x}^*$ that are attracted to it under the action of $\mathscr{P}$. They form an $(M-1)$-dimensional hypersurface $\mathscr{I}$, called an isochrone, crossing the limit cycle at $\mathbf{x}^*$ (see Fig. 1.5). A unique isochrone can be drawn through each point on the limit cycle so we can parameterize the isochrones by the phase, $\mathscr{I} = \mathscr{I}(\theta)$. Finally, we extend the definition of phase by taking all

points $\mathbf{x} \in \mathscr{I}(\theta)$ to have the same phase, $\Theta(\mathbf{x}) = \theta$, which then rotates at the natural frequency ω_0 (in the unperturbed case). Hence, for an unperturbed oscillator in the vicinity of the limit cycle, we have

$$\omega_0 = \frac{d\Theta(\mathbf{x})}{dt} = \sum_k \frac{\partial \Theta}{\partial x_k} \frac{dx_k}{dt} = \sum_k \frac{\partial \Theta}{\partial x_k} f_k(\mathbf{x}).$$

Now consider the perturbed system but with the unperturbed definition of the phase:

$$\frac{d\Theta(\mathbf{x})}{dt} = \sum_k \frac{\partial \Theta}{\partial x_k} (f_k(\mathbf{x}) + \varepsilon p_k(\mathbf{x},t)) = \omega_0 + \varepsilon \sum_k \frac{\partial \Theta}{\partial x_k} p_k(\mathbf{x},t).$$
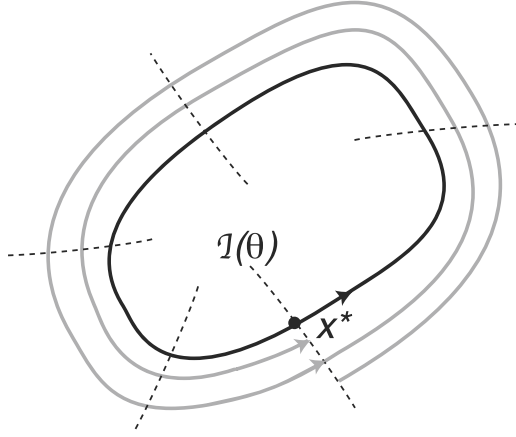
Fig. 1.5 Isochrones in the neighborhood of a stable limit cycle

To a first approximation we can neglect deviations of $\mathbf{x}$ from the limit cycle which we denote by $\mathbf{x}^*$:

$$\frac{d\Theta(\mathbf{x})}{dt} = \omega_0 + \varepsilon \sum_k \frac{\partial \Theta(\mathbf{x}^*)}{\partial x_k} p_k(\mathbf{x}^*,t).$$

Finally, since points on the limit cycle are in 1:1 correspondence with the phase θ, we obtain the closed phase equation

$$\frac{d\theta}{dt} = \omega_0 + \varepsilon Q(\theta,t), \tag{1.20}$$

where

$$Q(\theta,t) = \sum_k \frac{\partial \Theta(\mathbf{x}^*(\theta))}{\partial x_k} p_k(\mathbf{x}^*(\theta),t) \tag{1.21}$$

is a 2π-periodic function of θ and a Δ-periodic function of t.

Consider, as an example, the complex amplitude equation that arises for a limit cycle oscillator close to a Hopf bifurcation [248]:

$$\frac{dA}{dt} = (1 + i\eta)A - (1 + i\alpha)|A|^2 A, \quad A \in \mathbb{C}. \tag{1.22}$$

In polar coordinates $A = Re^{i\phi}$,

$$\frac{dR}{dt} = R(1 - R^2), \quad \frac{d\phi}{dt} = \eta - \alpha R^2.$$

The solution for arbitrary initial data $R(0) = R_0$, $\theta(0) = \theta_0$ is

$$R(t) = \left[1 + \frac{1 - R_0^2}{R_0^2} e^{-2t}\right]^{-1/2},$$

$$\phi(t) = \phi_0 + \omega_0 t - \frac{\alpha}{2} \log(R_0^2 + (1 - R_0^2)e^{-2t}), \tag{1.23}$$

where $\omega_0 = \eta - \alpha$ is the natural frequency of the stable limit cycle at $R = 1$. Strobing the solution at times $t = n\Delta_0$, we see that

$$\lim_{n \to \infty} \phi(n\Delta_0) = \phi_0 - \alpha \ln R_0.$$

Hence, we can define a phase on the whole plane

$$\Theta(R, \phi) = \phi - \alpha \ln R. \tag{1.24}$$

It follows that the isochrones are logarithmic spirals with $\phi - \alpha \ln R = $ constant. Now rewrite (1.22) in Cartesian coordinates

$$\frac{dx}{dt} = x - \eta y - (x^2 + y^2)(x - \alpha y) + \varepsilon \cos \omega t,$$

$$\frac{dy}{dt} = y + \eta y - (x^2 + y^2)(y + \alpha x),$$
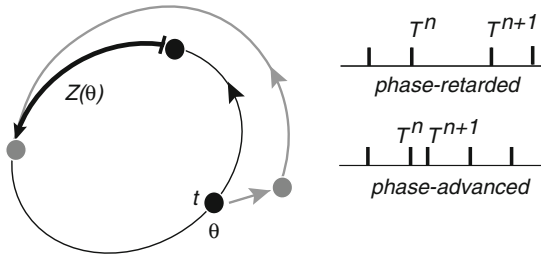
Fig. 1.6 Phase shift $Z(\theta)$ induced by a small perturbation of the membrane potential applied at time $t = 0$ when the phase of the limit cycle is θ. *Black (gray) dots* represent points on the unperturbed (perturbed) trajectory. The phase shift induces a corresponding shift in successive firing times

where we have added a periodic modulation in the x-direction. Rewrite the phase (1.24) as

$$\Theta = \tan^{-1}\frac{y}{x} - \frac{\alpha}{2}\log(x^2+y^2),$$

so that

$$\frac{\partial\Theta}{\partial x} = -\frac{y}{x^2+y^2} - \alpha\frac{x}{x^2+y^2}.$$

On the limit cycle $\mathbf{x}_0(\theta) = (\cos\theta,\sin\theta)$, we have

$$\frac{\partial\Theta(\mathbf{x}_0)}{\partial x} = -\sin\theta - \alpha\cos\theta.$$

It follows that the corresponding phase equation is

$$\frac{d\theta}{dt} = \omega_0 - \varepsilon(\alpha\cos\theta + \sin\theta)\cos\omega t.$$

The phase reduction method is particularly useful because the function $Q(\theta,t)$ can be related to an easily measurable property of a neural oscillator, namely, its *phase-resetting curve* (PRC), which we denote by the 2π-periodic function $Z(\theta)$. The PRC is found experimentally (or numerically) by perturbing the oscillator with a brief depolarizing voltage stimulus of size $\varepsilon\Delta V$ at different times in its cycle and measuring the resulting phase shift from the unperturbed system [221, 679]; see Fig. 1.6. Taking the coordinate x_1 as the membrane potential, it follows from (1.20) that

$$\frac{d\theta}{dt} = \omega_0 + \varepsilon\Delta x_1\frac{\partial\Theta(\mathbf{x}^*(\theta))}{\partial x_1}\delta(t-t_0). \tag{1.25}$$

Integrating this equation over a small interval around t_0, we see that the impulse induces a phase shift $\Delta\theta = (\varepsilon\Delta x_1)Z(\theta_0)$ where $Z(\theta) = \partial\Theta(\mathbf{x}^*(\theta))/\partial x_1$ and $\theta_0 = \theta(t_0)$. Thus comparing the phase at large times for the unperturbed and perturbed cases generates the PRC. Given the PRC $Z(\theta)$, the response of the neuron to a more general time-dependent voltage perturbation $\varepsilon P(t)$ is determined by the phase equation

$$\frac{d\theta}{dt} = \omega_0 + \varepsilon Z(\theta)P(t). \tag{1.26}$$

We can also express the PRC in terms of the firing times of a neuron (assuming fast reconvergence to the limit cycle). Suppose that there exists a well-defined threshold κ signaling the onset of fast somatic membrane depolarization and the subsequent firing of an action potential spike. Let T^n denote the nth firing time of the neuron as defined by (1.9). Since the membrane voltage $v(t) = x_1(\theta(t))$, the threshold corresponds to a particular phase of the limit cycle, which we choose to be $\theta = 0$. In the absence of perturbations, we have $\theta(t) = 2\pi t/\Delta_0$, so that the firing times are $T^n = n\Delta_0$ where Δ_0 is the natural period of oscillation. On the other hand, a small perturbation applied at the point θ on the limit cycle at time t, $T^n < t < T^{n+1}$, induces a phase shift that changes the next time of firing according to (see Fig. 1.6)
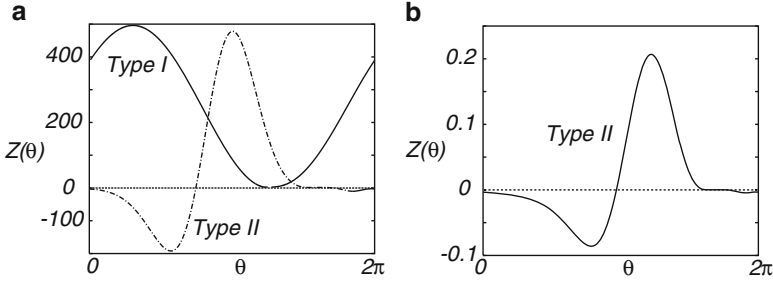
Fig. 1.7 (**a**) Morris–Lecar model showing two different response types. In both cases $v_k = -0.7$, $u_L = -0.5$, $u_{Ca} = 1$, $g_K = 2$, $g_L = 0.5$, $v_1 = -0.01$, $v_2 = 0.15$. For a type I response, $g_{Ca} = 1.33$, $v_3 = 0.1$, $v_4 = 0.145$, $\phi = 1/3$, and $I = 0.0695$. For a type II response, $g_{Ca} = 1.1$, $v_3 = 0$, $v_4 = 0.3$, $\phi = 0.2$, and $I = 0.25$. Responses have been scaled to the same ranges. (**b**) Hodgkin–Huxley model with external drive $I = 10$ showing type II phase-resetting curve

$$\frac{T^{n+1} - T^n}{\Delta_0} = 1 - \frac{(\varepsilon \Delta V) Z(\theta)}{2\pi}. \tag{1.27}$$

For certain types of neuron a depolarizing stimulus always advances the onset of the next spike, that is, the PRC is always positive, whereas for others the stimulus may also delay the next spike. Oscillators with a strictly positive PRC are called type I whereas those for which the PRC has a negative regime are called type II. A numerical example illustrating both types of PRC is shown in Fig. 1.7a for the Morris–Lecar model of a neuron, which was originally introduced to describe how under constant current injection barnacle muscle fibers respond with a host of oscillatory voltage waveforms [440]. It takes the form

$$\frac{\mathrm{d}v}{\mathrm{d}t} = I - g_L(v - v_L) - g_K w(v - v_K) - g_{Ca} m_\infty(v)(v - v_{Ca}),$$
$$\frac{\mathrm{d}w}{\mathrm{d}t} = \lambda(v)(w_\infty(v) - w), \tag{1.28}$$

with

$$m_\infty(v) = 0.5(1 + \tanh[(v - v_1)/v_2]),$$
$$w_\infty(v) = 0.5(1 + \tanh[(v - v_3)/v_4]),$$
$$\lambda(v) = \phi \cosh[(v - v_3)/(2v_4)].$$

Here, g_L is the leakage conductance, g_K, g_{Ca} are potassium and calcium conductances, v_L, v_K, v_{Ca} are corresponding reversal potentials, $m_\infty(v), w_\infty(v)$ are voltage-dependent gating functions, and $\lambda(v)$ is a voltage-dependent rate. The type II PRC for the Hodgkin–Huxley model is shown in Fig. 1.7b.

1.2.2 Phase-Locking and Synchronization

Now suppose that $Q(\theta, t)$ in (1.20) is expanded as a double Fourier series

$$Q(\theta,t) = \sum_{l,k} a_{l,k} e^{ik\theta + il\omega t}.$$

Substitute for θ using the zero-order approximation $\theta = \omega_0 t + \theta_0$:

$$Q(\theta,t) = \sum_{l,k} a_{l,k} e^{ik\theta_0 + i(k\omega_0 + l\omega)t}.$$

It follows that Q contains fast oscillating terms (compared to the time scale Δ_0/ε) together with slowly varying terms that satisfy the *resonance condition*

$$k\omega_0 + l\omega \approx 0. \tag{1.29}$$

Only the latter will lead to large variations in the phase, so we can average the forcing term Q keeping only the resonant terms. The simplest case is $\omega \approx \omega_0$ for which the resonant terms satisfy $l = -k$ and

$$Q(\theta,t) \to \sum_k a_{-k,k} e^{ik(\theta - \omega t)} = q(\theta - \omega t). \tag{1.30}$$

The phase equation then becomes

$$\frac{d\theta}{dt} = \omega_0 + \varepsilon q(\theta - \omega t).$$

The phase difference between the oscillator and external drive, $\psi = \theta - \omega t$, then satisfies the equation

$$\frac{d\psi}{dt} = -\Delta\omega + \varepsilon q(\psi), \tag{1.31}$$

where $\Delta\omega = \omega - \omega_0$ is the degree of *frequency detuning*. Similarly, if $\omega \approx m\omega_0/n$, then

$$Q(\theta,t) \to \sum_k a_{-nj,mj} e^{ij(m\theta - n\omega t)} = \hat{q}(m\theta - n\omega t), \tag{1.32}$$

and

$$\frac{d\psi}{dt} = m\omega_0 - n\omega + \varepsilon m\hat{q}(\psi), \tag{1.33}$$

where $\psi = m\theta - n\omega t$.

The above is an example of an application of the averaging theorem [248]. Assuming that $\Delta\omega = \omega - \omega_0 = \mathcal{O}(\varepsilon)$ and defining $\psi = \theta - \omega t$, we have

$$\frac{d\psi}{dt} = -\Delta\omega + \varepsilon Q(\psi + \omega t, t) = \mathcal{O}(\varepsilon). \tag{1.34}$$

Define

$$q(\psi) = \lim_{T \to \infty} \frac{1}{T} \int_0^T Q(\psi + \omega t, t) dt, \tag{1.35}$$

and consider the averaged equation

$$\frac{d\psi}{dt} = -\Delta\omega + \varepsilon q(\psi). \tag{1.36}$$

It is easy to establish that q only contains the resonant terms of Q as above. The averaging theorem ensures that there exists a change of variables that maps solutions of the full equation to those of the averaged equation to leading order in ε. The question then remains as to what extent solutions of the averaged equations are a good approximation to the solutions of the full equation. In general, one can only establish that a solution of the full equation is ε-close to a corresponding solution of the averaged system for times of $\mathcal{O}(\varepsilon^{-1})$. No such problem occurs however for hyperbolic fixed points corresponding to phase-locked states.

Suppose that the 2π-periodic function $q(\psi)$ has a unique maximum q_{max} and a unique minimum q_{min} in the interval $[0, 2\pi)$. We can then distinguish between two regimes [502]:

Synchronization regime: If the degree of detuning for a given drive amplitude is sufficiently small,

$$\varepsilon q_{min} < \Delta\omega < \varepsilon q_{\max},$$
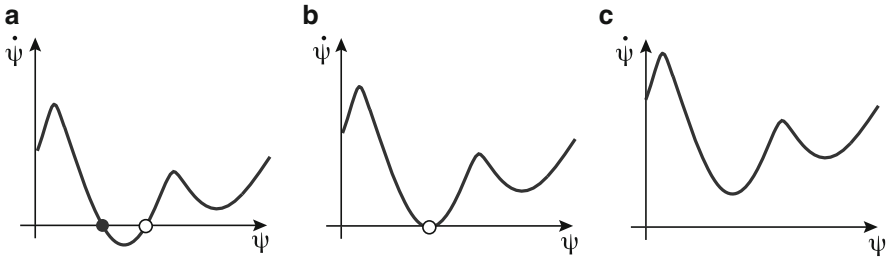
Fig. 1.8 Saddle–node bifurcation signaling a transition from a synchronized to a drifting state as the size of frequency detuning $|\Delta\omega|$ increases (**a**) Synchronization regime. (**b**) Saddle–node bifurcation. (**c**) Drift regime

then there exists at least one pair of stable/unstable fixed points (ψ_s, ψ_u). (This follows from the fact that $q(\psi)$ is 2π-periodic and continuous so it has to cross any horizontal line an even number of times.) The system evolves to the synchronized state

$$\theta(t) = \omega t + \psi_s,$$

in which the oscillator is *phase-locked* to the external drive and is *frequency entrained*. Note that the stability of a phase-locked state is determined by the sign of $q'(\psi)$ with $q'(\psi_s) < 0$ and $q'(\psi_u) > 0$ (see Fig. 1.8a).

Drift regime: As $|\Delta\omega|$ increases, it approaches one of the critical values $\varepsilon q_{min,max}$ where the two fixed points coalesce in a saddle–node bifurcation and phase-locking disappears; see Fig. 1.8b, c. Hence, if the degree of tuning is large, then $d\psi/dt$ never changes sign and the oscillation frequency differs from the drive frequency ω. The phase $\psi(t)$ rotates through 2π with period

$$T_\psi = \left| \int_0^{2\pi} \frac{d\psi}{\varepsilon q(\psi) - \Delta\omega} \right|. \tag{1.37}$$

The mean frequency of rotation is thus $\Omega = \omega + \Omega_\psi$ where $\Omega_\psi = 2\pi/T_\psi$ is known as the *beat frequency*. One is often interested in how the behavior varies in the $(\Delta\omega, \varepsilon)$-plane (see Fig. 1.9). First the boundary between the two regimes consists of the two straight lines $\Delta\omega = \varepsilon q_{max,min}$. Second, close to the boundary Ω_ψ has a characteristic form. Suppose, for example, that $\Delta\omega - \Delta\omega_{max}$ is small for fixed ε with $\Delta\omega_{max} = \varepsilon q_{max}$. The integral in (1.37) is then dominated by a small region around ψ_{max}. Expanding $q(\psi)$ as a Taylor series,

$$\Omega_\psi = \frac{2\pi}{T_\psi} \approx 2\pi \left| \int_{-\infty}^{\infty} \frac{d\psi}{\varepsilon q''(\psi_{max})\psi^2 - (\Delta\omega - \Delta\omega_{max})} \right|^{-1}$$

$$= \sqrt{\varepsilon |q''(\psi_{max})|(\Delta\omega - \Delta\omega_{max})}. \tag{1.38}$$
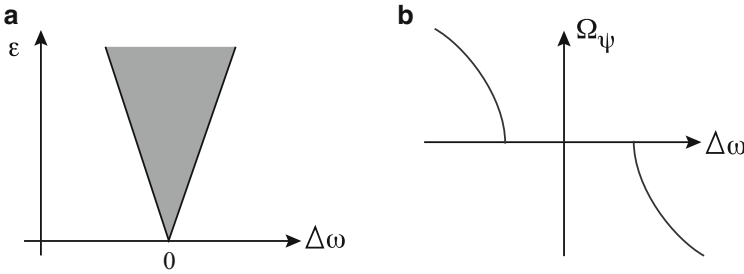
Fig. 1.9 (**a**) Synchronization regime (*shaded*) in $(\Delta\omega, \varepsilon)$-plane. (**b**) Variation of beat frequency with $\Delta\omega$ for fixed ε

1.3 Synaptic Processing

In the conductance-based model given by (1.6), we decomposed the total input current to the soma into an external part $I_{ext}(t)$ and a synaptic part $u(t)$. In this section, we consider the current generated at a single synapse and the sequence of events underlying conductance changes in the postsynaptic membrane due to the arrival of an action potential at the presynaptic terminal. We then show how these conductance changes can be modeled in terms of a kinetic scheme describing the opening and closing of ion channels in the postsynaptic membrane.

1.3.1 Excitatory and Inhibitory Synapses

The basic stages of synaptic processing induced by the arrival of an action potential
at an axon terminal are shown in Fig. 1.10. (See [99] for a more detailed description.)
An action potential arriving at the terminal of a presynaptic axon causes voltage-
gated Ca^{2+} channels within an active zone to open. The influx of Ca^{2+} produces
a high concentration of Ca^{2+} near the active zone [45, 195], which in turn causes
vesicles containing neurotransmitter to fuse with the presynaptic cell membrane and
release their contents into the synaptic cleft (a process known as exocytosis). The
released neurotransmitter molecules then diffuse across the synaptic cleft and bind
to specific receptors on the postsynaptic membrane. These receptors cause ion chan-
nels to open, thereby changing the membrane conductance and membrane potential
of the postsynaptic cell. A single synaptic event due to the arrival of an action po-
tential at time T induces a synaptic current of the form

$$I_{syn}(t) = g_{syn}(t - T)(V_{syn} - v(t)), \qquad (1.39)$$

where v is the voltage of the postsynaptic neuron, V_{syn} is the synaptic reversal po-
tential, and $g_{syn}(t)$ is the change in synaptic conductance with $g_{syn}(t) = 0$ for $t < 0$.
The sign of V_{syn} relative to the resting potential V_{rest} (typically $V_{rest} \approx -65\,mV$) de-
termines whether the synapse is excitatory ($V_{syn} > V_{rest}$) or inhibitory ($V_{syn} < V_{rest}$).
For simplicity, it is often assumed that a neuron spends most of its time close to rest
such that $V_{syn} - v \approx V_{syn} - V_{rest}$, with the factor $V_{syn} - V_{rest}$ absorbed into g_{syn}. One is
then effectively taking the arrival of a spike as generating a synaptic current rather
than a change in conductance.
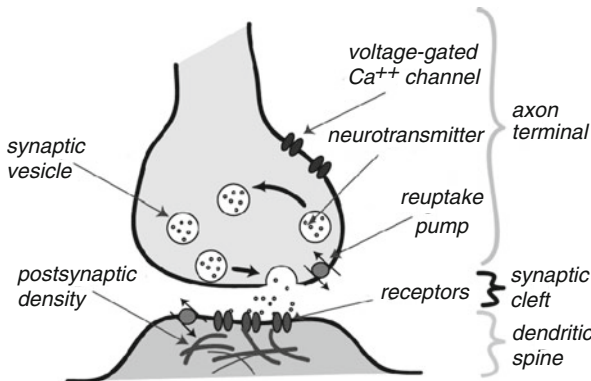
Fig. 1.10 Basic stages of synaptic processing shown for an excitatory synapse. See text for details

The predominant fast, excitatory neurotransmitter of the vertebrate central ner-
vous system is the amino acid *glutamate*, whereas in the peripheral nervous sys-
tem, it is *acetylcholine*. Glutamate-sensitive receptors in the postsynaptic mem-
brane can be subdivided into two major types, namely, NMDA and AMPA [99].

At an AMPA receptor the postsynaptic channels open very rapidly. The resulting increase in conductance peaks within a few hundred microseconds, with an exponential decay of around 1 ms. The time course of the synaptic conductance change can be modeled in terms of an nth state Markov process [154] (see Sect. 1.3.3). Usually a simplified representation of $g_{\text{syn}}(t)$ is used that is given by the difference of exponentials

$$g_{\text{syn}}(t) = \bar{g}\left(\frac{1}{\tau_2} - \frac{1}{\tau_1}\right)(e^{-t/\tau_1} - e^{-t/\tau_2})H(t), \qquad (1.40)$$

with $H(t)$ the Heaviside function. In many cases, the rise time is much shorter than the fall time ($\tau_1 \ll \tau_2$) so that we have an exponential synapse with $g_{\text{syn}}(t) = \bar{g}e^{-t/\tau_d}$. In the limit $\tau_2 \to \tau_1 = \alpha^{-1}$, (1.40) reduces to the well-known α function

$$g_{\text{syn}}(t) = \bar{g}\alpha^2 t e^{-\alpha t}H(t). \qquad (1.41)$$

These expressions for the conductance are also used for GABA inhibitory synapses (see below). In contrast to an AMPA receptor, the NMDA receptor operates about ten times slower and the amplitude of the conductance change depends on the postsynaptic membrane potential. If the postsynaptic potential is at rest and glutamate is bound to the NMDA receptor, then the channel opens, but it is physically obstructed by Mg^{2+} ions. As the membrane is depolarized, the Mg^{2+} ions move out and the channel becomes permeable to Na^+ and Ca^{2+} ions. The NMDA conductance can be derived from a model in which the binding rate constant of Mg^{2+} varies as an exponential function of the local voltage v [304]:

$$g_{\text{syn}}(t) = g\frac{e^{-t/\tau_1} - e^{-t/\tau_2}}{1 + \eta[Mg^{2+}]e^{-\gamma v(t)}}, \quad t > 0, \qquad (1.42)$$

where $[X]$ denotes concentration of X and η is a rate constant. The rapid influx of calcium ions due to the opening of NMDA channels is thought to be the critical trigger for the onset of *long-term potentiation* or LTP, a major component of synaptic plasticity (see also Sect. 4.1).

The most common inhibitory neurotransmitter in the central nervous system of both vertebrates and invertebrates appears to be GABA. There are two major forms of postsynaptic receptors termed A and B. The GABA$_A$ receptors open channels selective to chloride ions, whose reversal potential $V_{\text{syn}} = -70\,\text{mV}$ is close to that of the resting potential. The postsynaptic conductance change is quite fast, rising within 1 ms and decaying within 10–20 ms. GABA$_B$ receptors are at least 10 times slower and open ion channels selective for K^+ ions. Thus they tend to be considerably more hyperpolarizing with $V_{\text{syn}} \approx -100\,\text{mV}$. The two receptor classes tend to be segregated with GABA$_A$ occurring at or close to the soma and GABA$_B$ further out on the dendrites. Another way to distinguish between GABA$_A$ and GABA$_B$ receptors is that the former are *ionotropic* (as are NMDA and AMPA) while the latter are *metabotropic* [99]. Neurotransmitter binding to an ionotropic receptor directly opens an ion channel through a series of conformational changes of the receptor. On

the other hand, neurotransmitter binding to a metabotropic receptor indirectly opens an ion channel elsewhere in the membrane through a sequence of biochemical steps mediated by G proteins.

1.3.2 Synaptic Depression

A single synaptic event due to the arrival of an action potential at time T induces a synaptic current of the form (1.39). As a crude approximation we might try summing individual responses to model the synaptic current arising from a train of action potentials arriving at times T^m, integer m:

$$I_{\mathrm{syn}}(t) = \sum_m g_{\mathrm{syn}}(t - T^m)(V_{\mathrm{syn}} - v(t)). \qquad (1.43)$$

Note that this sum only includes spikes for which $T^m < t$ since $g_{\mathrm{syn}}(t) = 0$ for $t < 0$ (causality condition). For many synapses such a simple ansatz does not hold, since some form of short-term synaptic depression causes the amplitude of the response to depend on the previous history of presynaptic firing [4, 405]. One way to incorporate this history-dependent effect is to take [1]

$$I_{\mathrm{syn}}(t) = \left[\sum_m q(T^m) g_{\mathrm{syn}}(t - T^m) \right] (V_{\mathrm{syn}} - v(t)), \qquad (1.44)$$

where the factor $q(T^m)$ reduces the response evoked by an action potential by an amount that depends upon the details of the previous spike train data. One interpretation of the factor q is that it represents a short-term (reversible) reduction in the release probability for synaptic transmission due to a depletion in the number of vesicles that can readily fuse with the cell membrane [700]. In certain cases, it is also possible for a synapse to undergo a temporary facilitation in response to activation, which may be due to the presence of residual calcium in the axonal terminal [700].

A common phenomenological model of synaptic depression is to assume that between spikes $q(t)$ relaxes at a rate τ_q to its steady-state value of one, but that directly after the arrival of a spike it changes discontinuously, that is, $q \to \gamma q$ with $\gamma < 1$. The depression time constant τ_q can vary between around 100 ms and a few seconds [4]. The model for synaptic depression may be written succinctly as

$$\frac{dq}{dt} = \frac{(1-q)}{\tau_q} - (1-\gamma) \sum_n q(T^n) \delta(t - T^n), \quad q(0) = 1, \qquad (1.45)$$

which has the solution of the form

$$q(T^m) = 1 - (1-\gamma) \sum_{n<m} \gamma^{[m-n-1]\beta} \mathrm{e}^{-(T^m - T^n)/\tau_q}.$$

Assuming a regular sequence of incoming spikes $T^n - T^{n-1} = \Delta$ for all n we find that the asymptotic amplitude $q_\infty(\Delta) \equiv \lim_{m \to \infty} q(T^m)$ is given by

$$q_\infty(\Delta) = \frac{1 - e^{-\Delta/\tau_q}}{1 - \gamma e^{-\Delta/\tau_q}}. \tag{1.46}$$

One possible computational role for synaptic depression is as a mechanism for cortical gain control [4]. The basic idea can be understood from the dependence of the asymptotic amplitude $q_\infty(\Delta)$ on the stimulus frequency $f = \Delta^{-1}$. Assuming that $\tau_q \gg \Delta$, we can Taylor expand q_∞ in (1.46) to find that $q_\infty(f) \approx \Gamma/f$, where $\Gamma = \tau_q/(1 - \gamma)$. The main point to note is that the postsynaptic response per unit time is approximately independent of f (assuming that each spike elicits the same response in the steady state). This means that the synapse is very sensitive to changes in the stimulus frequency. The instantaneous response to a rapid increase Δf in the stimulus rate is given by $\Gamma \Delta f/f$. In other words, the synapse responds to relative rather than absolute changes in the rate of input stimulation.

1.3.3 Kinetic Model of a Synapse

Let $g_{\text{syn}}(t) \sim s(t)$ where $s(t)$ is the fraction of synaptic receptor channels that are in an open conducting state. The probability of being in an open state depends on the presence and concentration $\mathscr{T}$ of neurotransmitter released by the presynaptic neuron. Assuming a first-order kinetic scheme, in which a closed receptor in the presence of a concentration of neurotransmitter $\mathscr{T}$ equilibrates with the open receptor state, we have

$$C \underset{r_2(v)}{\overset{r_1(v,\mathscr{T})}{\rightleftharpoons}} O,$$
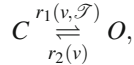
where C and O represent the closed and open states of the channel and $r_1(v, \mathscr{T})$ and $r_2(v)$ are the associated rate constants. However, in many cases synaptic channels are found to have time-dependent properties that are more accurately modeled with a second-order kinetic scheme. In fact the presence of one or more receptor sites on a channel allows the possibility of transitions to *desensitized states*. Such states are equivalent to the inactivated states of voltage-dependent ion channels. The addition of such a desensitized state to the first-order process generates a second-order scheme:

$$\frac{ds}{dt} = r_1(v, \mathscr{T})(1 - s - z) - [r_2(v) + r_3(v)]s + r_4(v)z,$$
$$\frac{dz}{dt} = r_6(v, \mathscr{T})(1 - s - z) - [r_4(v) + r_5(v)]z + r_3(v)s, \tag{1.47}$$

where z is the fraction of channels in the desensitized state. All neurotransmitter-dependent rate constants have the form $r_i(v, \mathscr{T}) = r_i(v)\mathscr{T}$. It is common for detailed Markov models of voltage-gated channels to assume that the voltage dependence

of all rates takes a simple exponential form. However, it has been shown that the number of states needed by a model to more accurately reproduce the behavior of a channel may be reduced by adopting sigmoidal functions for the voltage-dependent transition rates (see Destexhe et al. [154] for a discussion), so that we write

$$r_i(v) = \frac{a_i}{1 + \exp[-(v - c_i)/b_i]}. \tag{1.48}$$

The a_i set the maximum transition rate, b_i the steepness of the voltage dependence, and c_i the voltage at which the half-maximal rate is reached. Furthermore, the concentration of neurotransmitter can often be successfully approximated by a sigmoidal function of the presynaptic potential v_{pre}:

$$\mathscr{T}(v_{\text{pre}}) = \frac{\mathscr{T}_{\text{max}}}{1 + \exp[-(v_{\text{pre}} - v_\Delta)/\Delta]}. \tag{1.49}$$

Here, $\mathscr{T}_{\text{max}}$ is the maximal concentration of transmitter in the synaptic cleft, v_{pre} is the presynaptic voltage, Δ gives the steepness, and v_Δ sets the value at which the function is half activated. It is common to take $\Delta = 5\,\text{mV}$ and $v_\Delta = 2\,\text{mV}$. One of the main advantages of using an expression such as (1.49) is that it provides a smooth transformation between presynaptic voltage and transmitter concentration from which postsynaptic currents can easily be calculated from (1.39), (1.47), (1.48), and (1.49).

Now consider the following second-order gating scheme

$$
C \underset{r_2}{\overset{r_1(\mathscr{T})}{\rightleftharpoons}} C_1
$$
$$
\overset{r_4}{\nwarrow} \qquad \overset{}{\swarrow} r_3
$$
$$
O
$$
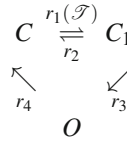
where C and C_1 are the closed forms of the receptor, O is the open (conducting) form, and the r_i are voltage-independent transition rates. Under certain assumptions it may be shown that this particular second-order scheme describes the so-called alpha function response commonly used in synaptic modeling. The following approximations are required: (i) The transmitter concentration $\mathscr{T}$ occurs as a pulse $\delta(t - t_0)$ for a release event occurring at time $t = t_0$, that is, $r_1(\mathscr{T}) = r_1\delta(t - t_0)$; (ii) The fraction of channels in C is considered constant and ~ 1. The kinetic equation (1.47) then reduce to

$$\frac{d\mathbf{c}(t)}{dt} = \mathbf{Q}\mathbf{c}(t) + \mathbf{I}(t),$$

(assuming $\mathbf{c}(0) = \mathbf{0}$), where

$$\mathbf{Q} = \begin{pmatrix} -\frac{1}{\tau_1} & 0 \\ r_3 & -\frac{1}{\tau_2} \end{pmatrix}, \quad \mathbf{I}(t) = \begin{pmatrix} r_1\delta(t - t_0) \\ 0 \end{pmatrix}, \quad \mathbf{c} = \begin{pmatrix} z \\ s \end{pmatrix},$$

and $\tau_1 = 1/(r_2 + r_3)$, $\tau_2 = 1/r_4$. Here z and s represent the fraction of receptors in the forms C_1 and O, respectively. This Markov chain system has a solution of the form

$$\mathbf{c}(t) = \int_0^t \mathbf{G}(t-s)\mathbf{I}(s)ds, \quad \mathbf{G}(t) = e^{t\mathbf{Q}}.$$

The eigenvectors of $\mathbf{Q}$ are $(1, r_3/(\tau_2^{-1} - \tau_1^{-1}))$ and $(0,1)$ with associated eigenvalues $-1/\tau_1$ and $-1/\tau_2$, respectively. Hence, one finds that

$$s(t) = r_1 r_3 \left(\frac{1}{\tau_2} - \frac{1}{\tau_1} \right)^{-1} (e^{-(t-t_0)/\tau_1} - e^{-(t-t_0)/\tau_2}), \quad t > t_0.$$

In the limit $\tau_2 \to \tau_1 \to \tau_s$ this reduces to an alpha function

$$s(t) = r_1 r_3 (t - t_0) e^{-(t-t_0)/\tau_s}, \quad t > t_0.$$

This kinetic derivation of the alpha function only holds for $s \ll 1$ in order to remain consistent with condition (ii).

The time course of some ion-channel open and closed states seems to follow a power law rather than multiexponential law at large times [429]. In order to understand such power-law behavior, consider an ion channel with N closed states such that the transition to an open state can only take place from state 1 at one end of a chain

$$0 \overset{\alpha}{\leftarrow} 1 \underset{\beta_1}{\overset{\gamma_1}{\rightleftharpoons}} 2 \ldots \underset{\beta_{N-1}}{\overset{\gamma_{N-1}}{\rightleftharpoons}} N.$$
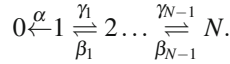
The corresponding kinetic equations are

$$\frac{dc_1}{dt} = \beta_1 c_2 - (\gamma_1 + \alpha)c_1,$$

$$\frac{dc_n}{dt} = \gamma_{n-1} c_{n-1} + \beta_n c_{n+1} - (\gamma_n + \beta_{n-1})c_n, \quad 1 < n < N,$$

$$\frac{dc_N}{dt} = \gamma_{N-1} c_{N-1} - \beta_{N-1} c_N.$$

In the following we take $\gamma_n = \beta_n = 1$ for all n and $\alpha = 1$, so that the system of equations describes a discrete diffusion process along a chain with a reflecting boundary at $n = N$ and an absorbing boundary at $n = 0$. In the large N limit, it can be shown that given the initial condition $p_n(0) = \delta_{n,1}$, the exact solution is

$$c_n(t) = e^{-2t}[I_{n-1}(t) - I_{n+1}(t)], \tag{1.50}$$

where $I_n(t)$ is the modified Bessel function of integer order:

$$I_n(t) = \int_{-\pi}^{\pi} e^{ink} e^{2t \cos(k)} \frac{dk}{2\pi}.$$

By carrying out an asymptotic expansion for large t, it can be shown that

$$c_n(t) \approx \frac{n}{2\pi^{1/2}t^{3/2}}.$$

Define $F(t)$ to be the total probability of finding the system in a closed state:

$$F(t) = \sum_{n=1}^{N} c_n(t).$$

It follows that $dF/dt = -\alpha c_1$ and, hence, $F(t) \approx (\pi t)^{-1/2}$ for large N, t and $\alpha = 1$. More recently, it has been suggested that synapses with multiple states, which exhibit dynamics over a wide range of time scales and show power-law-like behavior, could have some interesting computational properties [208, 219]. For example, it has been suggested that such synapses could provide a way of combining high levels of memory storage with long retention times [208].

1.4 Dendritic Processing

Typically, a single neuron in cerebral cortex has up to 10,000 synapses, which are spatially distributed along the dendritic tree (and perhaps on the cell body and proximal part of the axon). In order to find the total synaptic current $u(t)$ entering the cell body, it is necessary to determine how the various local currents flow along the dendritic tree and combine at the soma. We will show that if the dendrites are modeled as passive electrical cables, then the dendritic tree acts as a linear spatiotemporal filter of synaptic currents.

1.4.1 The Cable Equation

Neurons display a wide range of dendritic morphologies, ranging from compact arborizations to elaborate branching patterns. At the simplest level, the dendritic tree can be treated as a passive electrical medium that filters incoming synaptic stimuli in a diffusive manner. The current flow and potential changes along a branch of the tree may be described with a second-order, linear partial differential equation commonly known as the *cable equation*. (The application of cable theory to the study of passive, spatially extended dendrites was pioneered by Wilfrid Rall in the 1960s and 1970s. For more recent accounts of this work see [515] and the annotated collection of papers edited by Segev, Rinzel, and Shepherd [299].) The cable equation is based on a number of approximations: (1) magnetic fields due to the movement of electric charge can be neglected, (2) changes in ionic concentrations are sufficiently small so that Ohm's law holds, (3) radial and angular components of voltage can be ignored so that the cable can be treated as one-dimensional medium, and (4) dendritic membrane properties are voltage-independent, that is, there are no active elements.

A nerve cable consists of a long thin, electrically conducting core surrounded by a thin membrane whose resistance to transmembrane current flow is much greater than that of either the internal core or the surrounding medium. Injected current can travel long distances along the dendritic core before a significant fraction leaks out across the highly resistive cell membrane. Linear cable theory expresses conservation of electric current in infinitesimal cylindrical elements of nerve fiber modeled using the equivalent circuit shown in Fig. 1.11. Define $v(x,t)$ as the membrane potential at position x along a cable at time t (measured relative to the resting potential of the membrane). Let C_m be the capacitance per unit area of the cell membrane, R the resistivity of the intracellular fluid (in units of resistance $\times$ length), R_m the cell membrane resistance (in units of resistance $\times$ area), and a the cable radius. Note that C_m, R_m, R are independent of cable radius—the corresponding quantities expressed per unit length of cable are

$$r = \frac{R}{\pi a^2}, \quad \frac{1}{r_m} = \frac{2\pi a}{R_m}, \quad c_m = 2C_m\pi a. \tag{1.51}$$
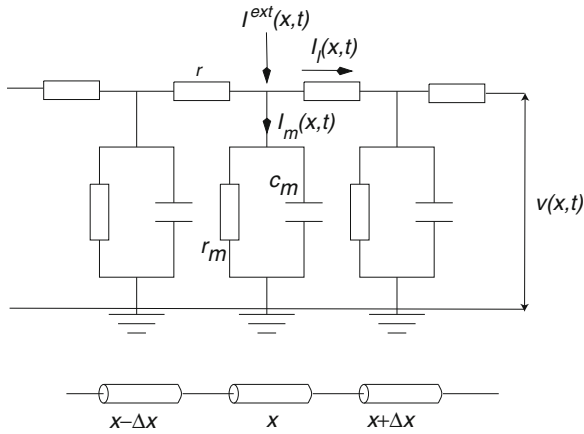
Fig. 1.11 Equivalent circuit for successive cylindrical segments of passive dendritic membrane

Current conservation implies that (see Fig. 1.11)

$$I^{ext}(x,t) - I_m(x,t) = \frac{I_l(x,t) - I_l(x-\Delta x,t)}{\Delta x} \approx \frac{\partial I_l(x,t)}{\partial x}, \tag{1.52}$$

where $I^{ext}(x,t)$ is an external injected current density. From Ohm's law we also have

$$I_l(x,t)r = \frac{v(x,t) - v(x+\Delta x,t)}{\Delta x} \approx -\frac{\partial v(x,t)}{\partial x}, \tag{1.53}$$

and

$$I_m(x,t) = c_m \frac{\partial v(x,t)}{\partial t} + \frac{v(x,t)}{r_m}. \tag{1.54}$$

Combining these three equations yields the uniform cable equation

$$\tau_m \frac{\partial v(x,t)}{\partial t} = -v(x,t) + \lambda_m^2 \frac{\partial^2 v(x,t)}{\partial x^2} + r_m I_{ext}(x,t), \qquad t \geq 0, \tag{1.55}$$

where $\tau_m = R_m C_m$ is the membrane time constant and $\lambda_m = (R_m a/2R)^{1/2}$ is the membrane space constant. (It follows that the coupling constant appearing in the Hodgkin–Huxley equation (1.8) is $K = \lambda_m^2/R_m$.)

Infinite Cable. In the case of an infinite uniform cable, $x \in \mathbb{R}$, we can solve (1.55) by Fourier transforming with respect to x. That is, define the Fourier transform of v (and other quantities) as

$$\tilde{v}(k,t) = \int_{-\infty}^{\infty} e^{-ikx} v(x,t) dx,$$

with inverse transform

$$v(x,t) = \int_{-\infty}^{\infty} e^{ikx} \tilde{v}(k,t) \frac{dk}{2\pi}.$$

Then

$$\tau_m \frac{\partial \tilde{v}(k,t)}{\partial t} = -\tilde{v}(k,t) - \lambda_m^2 k^2 \tilde{v}(k,t) + r_m \tilde{I}_{ext}(k,t), \quad x \in \mathbb{R}, \quad t \geq 0. \tag{1.56}$$

This first-order ODE can now be solved straightforwardly as

$$\tilde{v}(k,t) = \frac{r_m}{\tau_m} \int_{-\infty}^{t} \tilde{G}_0(k,t-t') \tilde{I}^{ext}(k,t') dt', \tag{1.57}$$

where $\tilde{G}_0(k,t) = e^{-(1+\lambda_m^2 k^2)t/\tau_m}$. Taking the inverse Fourier transform and using the convolution theorem shows that

$$v(x,t) = r_m \int_{-\infty}^{t} \left[\int_{-\infty}^{\infty} G_0(x-x',t-t') I^{ext}(x',t') dx' \right] dt', \tag{1.58}$$

where we have absorbed τ_m into r_m and

$$G_0(x,t) = \int_{-\infty}^{\infty} \frac{dk}{2\pi} e^{ikx} e^{-(1+\lambda_m^2 k^2)t/\tau_m}$$

$$= \frac{1}{2\lambda_m \sqrt{\pi t/\tau_m}} e^{-t/\tau_m} e^{-\tau_m x^2/4\lambda_m^2 t}. \tag{1.59}$$

The function $G_0(x,t)$ is the fundamental solution or Green's function for the cable equation with unbounded domain. It is positive and symmetric and satisfies the homogeneous cable equation

$$\left(\tau_m \frac{\partial}{\partial t} + 1 - \lambda_m^2 \frac{\partial^2}{\partial x^2} \right) G_0(x,t) = 0, \tag{1.60}$$

with initial condition

$$G_0(x,0) = \delta(x). \tag{1.61}$$

Moreover, for any $0 < s < t$, it satisfies the Markovian property

$$G_0(x-y,t) = \int_{-\infty}^{\infty} G_0(x-z,s)G_0(z-y,t-s)\mathrm{d}z. \tag{1.62}$$

The Green's function is plotted as a function of time in Fig. 1.12a for a range of separations x.

Semi-infinite Cable. Using Fourier cosine or sine transforms with respect to x it is straightforward to determine the Green's function for a semi-infinite cable $x \in [0, \infty)$ with either an open-end boundary condition

$$v(0,t) = 0 \tag{1.63}$$

or a closed-end boundary condition (zero current flow)

$$\left. \frac{\partial v(x,t)}{\partial x} \right|_{x=0} = 0 \tag{1.64}$$

One finds that

$$v(x,t) = r_m \int_{-\infty}^{t} \left[\int_0^{\infty} G_{\pm}(x,x',t-t')I^{ext}(x',t')dx' \right] dt' \tag{1.65}$$

where

$$G_{\pm}(x,y,t) = G_0(x-y,t) \pm G_0(x+y,t) \tag{1.66}$$

for the open $(-)$ and closed $(+)$ cases. For a discussion of finite-length cables see [342].

Single Branching Node. Let us now consider a single branching node and label each semi-infinite segment by the index $i = 1,\ldots,N$. (Typically $N = 3$.) We shall assume that the cables only differ in their radius a_i. In order to simplify the analysis we will measure the distance along the ith cable from the branch point at $x = 0$ in units of $\lambda_{m,i} = \sqrt{R_m a_i / 2R}$ such that the cable equation on each branch can be written as

$$\tau_m \frac{\partial v_i(X,t)}{\partial t} = -v_i(x,t) + \frac{\partial^2 v_i(x,t)}{\partial x^2} + I_i(x,t). \tag{1.67}$$

The boundary conditions are continuity of the potential at the node

$$v_i(0,t) = v_j(0,t), \tag{1.68}$$

and conservation of current
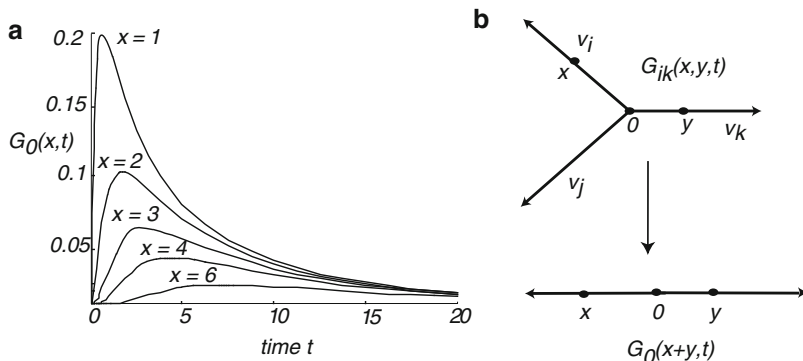
Fig. 1.12 (**a**) Green's function of an infinite cable as a function of time t (in units of τ_m) for various values of distance x (in units of λ). (**b**) Branching dendritic tree of an idealized single neuron and an equivalent cylinder representation

$$\sum_{j=1}^{N} a_j^{3/2} \left. \frac{\partial v_j(x,t)}{\partial x} \right|_{x=0} = 0. \tag{1.69}$$

The factor $a_i^{3/2}$ arises from the fact that we have rescaled length and that the longitudinal resistance varies as the cross-sectional area of the cable. The solution of these equations is

$$v_i(x,t) = \sum_{j=1}^{N} \int_{-\infty}^{t} \left[\int_0^{\infty} G_{ij}(x,x',t-t') I_j(x',t') dx' \right] dt', \tag{1.70}$$

where

$$G_{ij}(x,y,t) = \delta_{i,j} G_0(x-y,t) + (2p_j - \delta_{i,j}) G_o(x+y,t), \tag{1.71}$$

and

$$p_k = \frac{a_k^{3/2}}{\sum_m a_m^{3/2}}. \tag{1.72}$$

It is interesting to note that if $p_k = 1/2$ for a certain segment, then the response to current injected into that segment can be represented by a single equivalent cylinder; see Fig. 1.12b. That is, if $i \neq j$, then $G_{ij}(x,y,t) = G_0(x+y)$, where $x+y$ is the distance of the direct path between x and y on the tree. Hence, the node in some sense acts no differently than an ordinary point on a single cable. This is the basis of Rall's equivalent cylinder concept [515].

Dendritic Tree. An arbitrary dendritic tree Γ may be considered as a set of branching nodes linked by finite pieces of uniform cable. Given an external current density $I^{ext}(x,t)$ the voltage response has the formal solution (absorbing r_m into the definition of G)

$$v(x,t) = \int_{-\infty}^{t} \left[\int_{\Gamma} G(x,y,t-s)I_{\text{ext}}(y,s)dy \right] ds. \qquad (1.73)$$

The associated Green's function $G(x,y,t-s)$ satisfies the homogeneous cable equation on each segment together with boundary conditions at the branching and terminal nodes of the tree. Rules for constructing such a Green's function have been developed by Butz and Cowan [95] using a graphical calculus and by Abbott et al. [3] using path-summing methods. The latter approach can be understood in terms of a compartmental model obtained by spatially discretizing the cable equation. The construction of the discretized Green's function involves summing over paths of a random walk on the tree with the corresponding Green's function for the cable equation recovered in the continuum limit [77].

1.4.2 Dendritic Filtering of Synaptic Inputs

So far we have considered the linear response of a dendritic cable to external current injection as determined by the Green's function or transfer function. Suppose that we replace the external current by a synaptic current of the form discussed in Sect. 1.3. That is, $I_{\text{ext}}(x,t) \to I(x,t)$, where $I(x,t)$ is the synaptic current density at location x at time t:

$$I(x,t) = \rho(x) \sum_m g_{\text{syn}}(t - T^m(x))[V_{\text{syn}} - v(x,t)] \equiv g(x,t)[V_{\text{syn}} - v(x,t)], \qquad (1.74)$$

where $g(x,t) = \rho(x) \sum_m g_{\text{syn}}(t - T^m(x))$. Here $\rho(x)$ is the density of synapses (assuming that they have identical properties) and $\{T^m(x)\}$ is the sequence of spikes arriving into the synapses located at x. In the case of a discrete set of identical synapses at dendritic locations $\{x_j, j = 1, \ldots, M\}$, we have $\rho(x) = \sum_j \delta(x - x_j)$ and $T^m(x_j) = T_j^m$. The formal solution for the membrane potential is now [see (1.73)]

$$v(x,t) = \int_{-\infty}^{t} \left[\int_{\Gamma} G(x,x',t-t')g(x',t')[V_{\text{syn}} - v(x',t')]]dx' \right] dt' \qquad (1.75)$$

which is a Volterra integral equation of the second kind. In order to solve this integral equation, we introduce the convolution operator $*$,

$$[G*f](x,t) := \int_{-\infty}^{t} \left[\int_{\Gamma} G(x,x',t-t')f(x',t')dx' \right] dt' \qquad (1.76)$$

for any function $f(x,t)$. We can then iterate (1.75) to obtain a series solution for v:

$$v = V_{\text{syn}}G*g - G*(gv)$$
$$= V_{\text{syn}}G*g - V_{\text{syn}}G*(g[V_{\text{syn}}G*g - G*(gv)])$$
$$= V_{\text{syn}}G*g - V_{\text{syn}}^2G*[gG*g] + G*[gG*(gv)]$$

$$= V_{\text{syn}}G*g - V_{\text{syn}}^2 G*(gG*g) + V_{\text{syn}}^3 G*(gG*[gG*g]) - \dots$$
$$= V_{\text{syn}}(G - V_{\text{syn}}G*gG + V_{\text{syn}}^2 G*gG*gG - \dots)*g$$
$$= V_{\text{syn}}\hat{G}*g, \tag{1.77}$$

where

$$\hat{G} := G - V_{\text{syn}}G*gG + V_{\text{syn}}^2 G*gG*gG - \dots \tag{1.78}$$

is a Neumann series expansion for the effective Green's function $\hat{G}$, which is convergent for a passive cable [344]. More explicitly, we can write the solution as

$$v(x,t) = V_{\text{syn}} \int_{-\infty}^{t} \left[\int_{\Gamma} \hat{G}(x,t;x',t')g(x',t')dx' \right] dt', \tag{1.79}$$
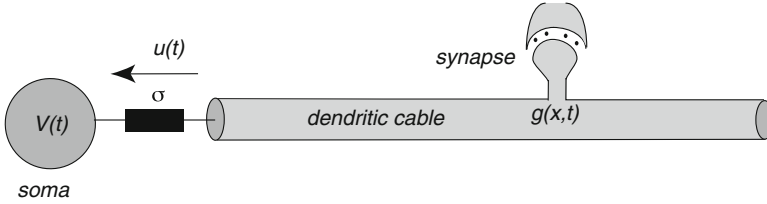
Fig. 1.13 Schematic diagram of a neuron consisting of a soma resistively coupled to one end of a dendritic cable. A synaptic conductance change $g(x,t)$ at position x on the cable induces a synaptic current into the soma at $x = 0$

with $\hat{G}$ satisfying the Volterra integral equation

$$\hat{G}(x,t;x',t') = G(x,x',t-t') \tag{1.80}$$
$$- V_{\text{syn}} \int_{t'}^{t} \left[\int_{0}^{\infty} G(x,x'',t-t'')g(x'',t'')\hat{G}(x'',t'';x',t')dx'' \right] dt''.$$

One can check that iteration of this equation recovers the series expansion for $\hat{G}$. The major point to note is that the resulting series involves interactions between synaptic conductances at different points on the dendritic cable. For simplicity, however, we shall assume that $V_{\text{syn}} \gg v(x,t)$ so that $\hat{G} \to G$ and synaptic interactions become negligible.

Given a distribution of synaptic inputs innervating the dendritic tree, what is the net synaptic current $u(t)$ entering the soma? In order to address this problem, consider a semi-infinite uniform dendritic cable, $0 \le x < \infty$, with the soma located at the end $x = 0$. The soma is modeled as a conductance-based point process that is passively coupled to the dendritic cable as illustrated in Fig. 1.13:

$$C\frac{dv}{dt} = -I_{\text{con}} + \sigma[v(0,t) - v(t)], \tag{1.81}$$

and

$$\tau_m \frac{\partial v(x,t)}{\partial t} = -v(x,t) + \lambda_m^2 \frac{\partial^2 v(x,t)}{\partial x^2} + r_m V_{syn} g(x,t). \tag{1.82}$$

Here $u(t) = \sigma[v(0,t) - v(t)]$ is the net current density flowing into the soma from the dendritic cable at $x = 0$. (We are neglecting direct synaptic inputs into the soma.) Current conservation implies the boundary condition

$$-\frac{1}{r}\frac{\partial v}{\partial x}(0,t) = \sigma[v(0,t) - v(t)]. \tag{1.83}$$

Since we can eliminate the term $-\sigma v(t)$ in (1.81) by shifting the linear term in v, it follows that the total synaptic current into the soma is $u(t) = \sigma v(0,t)$.
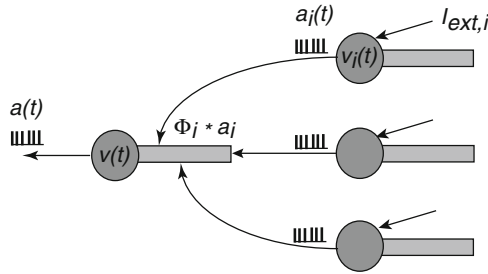
Fig. 1.14 Schematic diagram of a feedforward network showing a set of afferent neurons labeled by i synaptically driving another neuron

The inhomogeneous boundary problem for $v(0,t)$ can be solved formally using the Green's function G_+ for the semi-infinite cable with a closed boundary:

$$v(0,t) = r_m V_{syn} \int_{-\infty}^{t} \left[\int_0^\infty G_+(0,x',t-t')g(x',t')dx' \right] dt'$$

$$- \sigma r \int_{-\infty}^{t} G_+(0,0,t-t')[v(0,t') - v(t')]dt' \tag{1.84}$$

This shows that the effective synaptic current $u(t)$ flowing into the soma will itself be affected by the cell firing an action potential, due to the dependence of $v(0,t)$ on the somatic potential $v(t)$. However, suppose that the second term on the r.h.s. is negligible compared to the first term arising from synaptic inputs. This approximation corresponds to imposing the homogeneous boundary condition $\partial v/\partial x(0,t) = 0$. It then follows that the total synaptic input into the soma is

$$u(t) = \sigma r_m V_{syn} \int_{-\infty}^{t} \left[\int_0^\infty G_+(0,x',t-t')g(x',t')dx' \right] dt' \tag{1.85}$$

A similar analysis can also be carried out for more general dendritic topologies with the soma coupled to one of the terminals of the tree. We conclude that under the

given approximations, the passive dendritic tree acts like a spatiotemporal linear filter on incoming spike trains, whose properties are determined by the underlying Green's function on the tree.

Recall from (1.74) that $g(x,t) = \rho(x)\sum_m g_{\text{syn}}(t - T^m(x))$. Suppose that there exists a discrete set of synapses along the dendrite so that $\rho(x) = \sum_j \delta(x - x_j)$ and $T^m(x_j) = T_j^m$. Substituting into (1.85) then gives

$$u(t) = \sum_j \sum_m \Phi_j(t - T_j^m) = \sum_j \int_{-\infty}^t \Phi_j(t - t')a_j(t')dt', \qquad (1.86)$$

where

$$\Phi_j(t) = \sigma r_m V_{\text{syn}} \int_0^t G_+(0, x_j, t - \tau)g_{\text{syn}}(\tau)d\tau, \qquad (1.87)$$

and

$$a_j(t) = \sum_m \delta(t - T_j^m). \qquad (1.88)$$

Note that $a_j(t)$ represents the spike train arriving into the jth synapse in terms of a sum of Dirac delta functions. Hence, under our various approximations, we can view the total synaptic input $u(t)$ as the sum of linearly filtered spike trains, with the kernel of each filter determined by synaptic and dendritic processing. Now suppose that each incoming spike train is associated with a distinct afferent neuron, so that there is a one-to-one correspondence between synaptic and afferent neuron labels; see Fig. 1.14. Then $T_j^m = \hat{T}_j^m + \Delta \tau_j$, where $\hat{T}_j^m$ is the mth firing time of the jth afferent neuron and $\Delta \tau_j$ is an axonal propagation time delay. Unless stated otherwise, we will ignore axonal propagation delays and set $T_j^m = \hat{T}_j^m$. Let us also assume that each afferent neuron is described by a conductance-based model of the form

$$C_i \frac{dv_i}{dt} = -I_{\text{con},i} + I_{\text{ext},i} \qquad (1.89)$$

where v_i is the somatic membrane potential of the ith afferent neuron, each of which is driven by an external input $I_{\text{ext},i}$. If we associate with each neuron a firing threshold κ, then the spike times T_i^m are determined according to

$$T_i^m = \inf\{t, t > T_i^{m-1} | v_i(t) = \kappa, \dot{v}_i(t) > 0\}. \qquad (1.90)$$

Finally, given $u(t)$, the spike train $a(t)$ of the output neuron is determined by (1.1) and (1.9). In summary, the feedforward network involves a mapping $\{I_{\text{ext},i}(t)\} \to \{T_i^m\} \to \{T^m\}$.

1.4.3 Active Dendrites

It has been known for more than twenty years that the dendrites of cortical neurons do not simply act as passive electrical cables but also exhibit a variety of

active physiological processes [608]. For example, thick apical dendrites of pyramidal neurons express voltage-gated Na^+, K^+, and Ca^{2+} channels, which support the back propagation of action potentials (APs) from the soma into the dendritic tree [397, 606]; back-propagating APs are thought to play an important role in spike-timing-dependent synaptic plasticity (STDP) [585]. In addition, sufficient local stimulation of active apical dendrites can initiate regenerative membrane depolarizations known as *dendritic spikes* [333, 555]. Some dendritic spikes are restricted to the local initiation zone rather than invading the cell body and are thus well placed to mediate the long-term potentiation of synaptic inputs in the absence of output spiking of the neuron [226]. On the other hand, Ca^{2+} action potentials initiated in apical dendrites can propagate towards the soma, which provides a mechanism for actively amplifying the effects of distal synapses on AP generation in the cell body [361]. Following advances in imaging techniques and methods of dendritic stimulation, Schiller et al. [556] established in vitro that active processes can also occur in thin basal and apical dendritic branches of pyramidal neurons, where the majority of synapses occur; see Fig. 1.15a. In particular, they found stimulus-evoked dendritic spikes whose major ionic component involved ligand-gated and voltage-gated N-methyl-D-aspartate receptor (NMDAR) channels; see also [362, 400, 520] and the review [12]. When glutamate binds to an NMDAR, it modifies the voltage sensitivity of the corresponding ion-channel current, which develops a negative slope conductance due to removal of a magnesium block [414, 466]. This means that in the presence of high levels of glutamate, the current–voltage (I–V) characteristics of an NMDAR channel are very similar to the voltage-gated Na channel. Hence, during
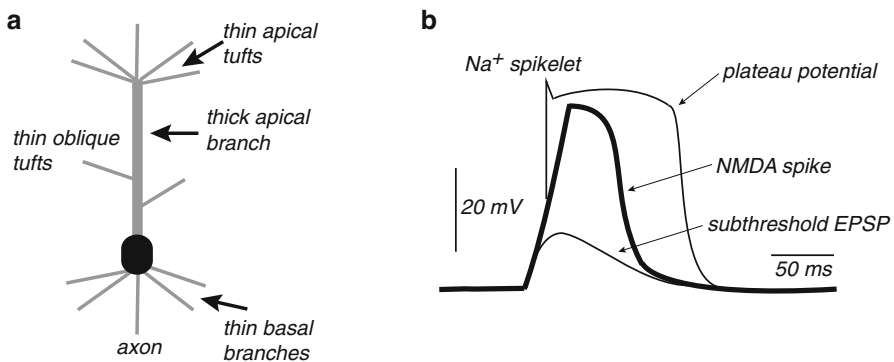
Fig. 1.15 (**a**) Schematic illustration of a pyramidal neuron showing the thick apical dendrite and various thin dendrites. The latter support the initiation of dendritic NMDA spikes. (**b**) Typical waveform of a dendritic NMDA spike. Weak glutamatergic inputs generate EPSP-like (subthreshold) depolarizations. A stronger input can trigger a dendritic plateau potential, consisting of a rapid onset that is often associated with a Na spikelet, a long-lasting plateau phase that can have a duration of several hundred ms, and a sudden collapse at the end of the plateau phase. The plateau potential consists of several dendritic conductances, the most predominant being due to NDMAR channels. Pharmacologically blocking Na and Ca^{2+} channels reveals the pure dendritic NMDA spike [556]

strong stimulation of a thin dendrite due to the local uncaging of glutamate or high frequency stimulation of a cluster of synapses, the NMDARs can fire a regenerative dendritic spike, just as Na channels support the initiation of an action potential following membrane depolarization. However, the duration of the dendritic spike is of the order 100 ms rather than 1 ms; see Fig. 1.15b. Finally, active processes can also be found in dendritic spines, which can support the propagation of saltatory waves; see Sect. 3.1

For relatively small deviations of the membrane potential from some constant value, a linearization of the channel kinetics can be performed. The resulting system has a membrane impedance that displays resonant-like behavior due to the additional presence of effective inductances [61, 141, 341, 342]. We sketch how inductance-like behavior can arise from active neural membrane by considering a generic ion current of the form $I(v, x_1, \ldots, x_M)$, where v is membrane voltage and x_k are gating variables that satisfy

$$\tau_k(v)\frac{dx_k}{dt} = x_{k,\infty}(v) - x_k, \quad k = 1, \ldots, M. \tag{1.91}$$

It is convenient to set $\tau_k(v) = (\alpha_k(v) + \beta_k(v))^{-1}$ and $x_{k,\infty}(v) = \alpha_k(v)\tau_k(v)$. Linearizing around a fixed point $\mathbf{z} = \mathbf{z}^*$ with vectors defined by $\mathbf{z} = (v, x_1, \ldots, x_M)^T$ and $\mathbf{z}^* = (v^*, x_{1,\infty}(v^*), \ldots, x_{M,\infty}(v^*))$, we have

$$\delta I = \frac{\delta v}{R} + \sum_{k=1}^{M} \left.\frac{\partial I}{\partial x_k}\right|_{\mathbf{z}=\mathbf{z}^*} \delta x_k, \tag{1.92}$$

where R is an effective resistance such that $R^{-1} = \partial I/\partial V|_{\mathbf{z}=\mathbf{z}^*}$. From (1.91) it follows that

$$\left(\frac{d}{dt} + \alpha_k + \beta_k\right)\delta x_k = \left(\frac{d\alpha_k}{dV} - x_{k,\infty}\frac{d[\alpha_k + \beta_k]}{dV}\right)\delta V_k. \tag{1.93}$$

Combining (1.92) and (1.93) we arrive at the following equation for the first-order variation of the current:

$$\delta I = \frac{\delta V}{R} + \sum_{k=1}^{M} \delta I_k, \tag{1.94}$$

where

$$\left(r_k + L_k\frac{d}{dt}\right)\delta I_k = \delta V, \tag{1.95}$$

and

$$r_k^{-1} = \tau_k \frac{\partial I}{\partial x_k}\left(\frac{d\alpha_k}{dV} - x_{k,\infty}\frac{d[\alpha_k + \beta_k]}{dV}\right)\Bigg|_{\mathbf{z}=\mathbf{z}^*} \tag{1.96}$$

$$L_k = \tau_k r_k \tag{1.97}$$

Hence, for a small perturbation around the steady state, the current I responds as though the resistance R is in parallel with M impedance lines, each of which is a resistance r_k that is itself in series with an inductance L_k (see Fig. 1.16). Such inductive terms account for the oscillatory *overshoot* commonly seen in response to depolarising current steps or even after the firing of an action potential. This form of equivalent linear membrane circuit is typically called *quasi-active* in order to distinguish it from a truly *active* (i.e. nonlinear) membrane [341].
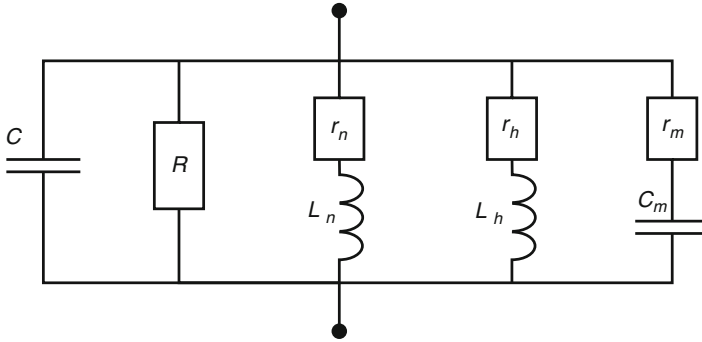
Fig. 1.16 Electrical LRC circuit representing the linearized response of the Hodgkin–Huxley equations

Quasilinear membrane can be incorporated into the cable equation (1.55) by introducing the space-dependent voltage $v(x,t)$ and currents $I_k(x,t)$, $x \in \mathbb{R}$, such that

$$\frac{\partial V}{\partial t} = -\frac{V}{\tau_m} + D_m \frac{\partial^2 V}{\partial x^2} - \frac{1}{C_m}\left[\sum_k I_k - I_{\text{ext}}\right] \tag{1.98a}$$

$$L_k \frac{dI_k}{dt} = -r_k I_k + V. \tag{1.98b}$$

Here $D_m = \lambda_m^2/\tau_m$. Laplace transforming (1.98) with $v(x,0) = 0, I_k(x,0) = 0$ yields the ODE

$$-\frac{d\tilde{V}^2}{dx^2} + \gamma^2(\omega)\tilde{V} = \tilde{I}, \tag{1.99}$$

with $\tilde{V} = \tilde{V}(x,\omega)$, $\tilde{I} = \tilde{I}(x,\omega) = \tilde{I}_{\text{ext}}(x,\omega)/C_m$, and

$$\gamma^2(\omega) = \frac{1}{D_m}\left[\frac{1}{\tau_m} + \omega + \frac{1}{C_m}\sum_k \frac{1}{r_k + \omega L_k}\right]. \tag{1.100}$$

It follows that in Laplace space,

$$\tilde{V}(x,\omega) = \int_0^\infty \tilde{G}(x-y,\omega)\tilde{I}(y,\omega)dy, \quad \tilde{G}(x,\omega) = \frac{e^{-\gamma(\omega)|x|}}{2D_m\gamma(\omega)}, \tag{1.101}$$

where $\tilde{G}$ is the Laplace transform of the Green's function on an infinite quasi-active cable. Having obtained G, it is then possible to extend Green's function methods outlined for passive branching cables to the quasi-active case [141].

1.5 Stochastic Ion Channels

In the standard conductance-based model of a neuron (1.6), it is assumed that the number of voltage-gated ion channels is sufficiently large so that one can represent the opening and closing of the channels in terms of deterministic kinetic equations. These keep track of the fraction of open and closed channels as a function of time. However, the opening and closing of a single channel is a stochastic process. This then raises the important issue of how such stochasticity manifests itself when there are relatively few ion channels. (A similar issue applies to synapses with a small number of receptor-mediated ion channels.) In this section, we develop the theory of stochastic ion channels in some detail, since it provides an excellent platform for introducing various methods and ideas in stochastic processes that will be used throughout the book. For reviews on noise in ion channels see [227, 588, 670].

1.5.1 Ensemble of Two-State Ion Channels

First, consider a single ion channel that can exist either in a closed state (C) or an open state (O). Transitions between the two states are governed by a continuous-time jump Markov process

$$C(\text{closed}) \underset{\beta(v)}{\overset{\alpha(v)}{\rightleftharpoons}} O(\text{open}). \tag{1.102}$$

with voltage-dependent transition rates $\alpha(v), \beta(v)$. For the moment, we assume that v is fixed. In order to understand what such a process means, let $Z(t)$ be a discrete random variable taking values $Z \in \{C, O\}$ and set $P_z(t) = \text{Prob}[Z(t) = z]$. From conservation of probability,

$$P_C(t) + P_O(t) = 1.$$

The transition rates then determine the probability of jumping from one state to the other in a small interval Δt:

$$\alpha \Delta t = \text{Prob}[Z(t + \Delta t) = O | Z(t) = C], \quad \beta \Delta t = \text{Prob}[Z(t + \Delta t) = C | Z(t) = O].$$

It follows that there are two possible ways for the ion channel to enter or leave the closed state:

$$P_C(t + \Delta t) = P_C(t) - \alpha P_C(t) \Delta t + \beta P_O(t) \Delta t.$$

Writing down a similar equation for the open state, dividing by Δt, and taking the limit $\Delta t \to 0$ leads to the pair of equations

$$\frac{dP_C}{dt} = -\alpha P_C + \beta P_O \tag{1.103a}$$

$$\frac{dP_O}{dt} = \alpha P_C - \beta P_O. \tag{1.103b}$$

Now suppose that there are N identical, independent two-state ion channels. In the limit $N \to \infty$ we can reinterpret P_C and P_O as the mean fraction of closed and open ion channels within the population, and fluctuations can be neglected. After setting $P_O = X$ and $P_C = 1 - X$, we recover the kinetic equation (1.4). (An identical argument can be applied to the kinetic model of a synapse considered in Sect. 1.3.)

In order to take into account fluctuations in the case of finite N, it is necessary to keep track of the probability $P(n,t)$ that there are n open channels at time t, $0 \le n \le N$. (If there are n open channels, then it immediately follows that there are $N - n$ closed channels, so we do not need to keep track of the latter as well.) Consider a time interval $[t, t+\Delta t]$ with Δt sufficiently small so that only one channel has a significant probability of making a $C \to O$ or $O \to C$ transition. There are four possible events that can influence $P(n,t)$ during this interval, two of which involve transitions into the state of n open ion channels, and two of which involve transitions out of the state. Collecting these terms and taking the limit $\Delta t \to 0$ leads to the *master equation*

$$\frac{d}{dt}P(n,t) = \alpha(N-n+1)P(n-1,t) + \beta(n+1)P(n+1,t) - [\alpha(N-n) + \beta n]P(n,t). \tag{1.104}$$

The first term on the right-hand side represents the probability flux that one of $N - (n-1)$ closed channels undergoes the transition $C \to O$, whereas the second term represents the probability flux that one of $n + 1$ open channels undergoes the transition $O \to C$. The last two terms represent transitions $n \to n \pm 1$. Define the mean number of open channels at time t by

$$\bar{n}(t) = \sum_{n=0}^{N} nP(n,t).$$

By differentiating both sides of this equation with respect to t and using the master equation (1.104), it can be shown that in the limit of large N (where the upper limit in the sum can be taken to be ∞) we recover the kinetic equation (1.4) with $X = \bar{n}/N$.

The steady-state solution $P_s(n)$ of the master equation (1.104) satisfies $J(n) = J(n+1)$ with

$$J(n) = \omega_-(n)P_s(n) - \omega_+(n-1)P_s(n-1),$$

and
$$\omega_+(n) = (N-n)\alpha, \quad \omega_-(n) = n\beta.$$

Using the fact that n is a nonnegative integer, that is, $P_s(n) = 0$ for $n < 0$, it follows that $J(n) = 0$ for all n. Hence, by iteration,

$$P_s(n) = P_s(0) \prod_{m=1}^{n} \frac{\omega_+(m-1)}{\omega_-(m)} = P_s(0) \left[\frac{\alpha}{\beta}\right]^n \frac{N!}{n!(N-n)!}. \tag{1.105}$$

Taking logs of both sides of this equation and using Stirling's formula $\log(n!) \approx n\log n - n$ it can be shown that for large n, N, $P_s(n) \approx p_s(x)$ where $x = n/N$,

$$p_s(x) = \mathcal{N}e^{-N\Phi(x)} \tag{1.106}$$

with normalization factor $\mathcal{N}$ and $\Phi(x)$ is the effective potential

$$\Phi(x) = -x\log(\alpha/\beta) + x\log(x) + (1-x)\log(1-x). \tag{1.107}$$

Let x^* be the unique critical point of the effective potential $\Phi(x)$, that is, $\Phi'(x^*) = 0$. Note that x^* coincides with the fixed point of the corresponding deterministic kinetic equations,

$$x^* = \frac{\alpha}{\alpha + \beta}. \tag{1.108}$$

Since N is large, we can make the Gaussian approximation

$$p_s(x) \approx p(0)\exp\left[-N\Phi(x^*) - N\Phi''(x^*)(x-x^*)^2/2\right]. \tag{1.109}$$

Under this approximation, the mean and variance of the fraction of open channels are given by

$$\frac{\bar{n}}{N} = x^* = \frac{\alpha}{\alpha+\beta}, \quad \frac{\langle(n-\bar{n})^2\rangle}{N^2} = \frac{x^*(1-x^*)}{N}. \tag{1.110}$$

It is clear that fluctuations become negligible in the large-N limit.

1.5.2 Diffusion Approximation

A useful diffusion approximation of the master equation (1.104) for large but finite N can be obtained by carrying out a Kramers–Moyal or system-size expansion to second order in N^{-1} [210, 309], which was originally applied to ion-channel models by Fox and Lu [200]. This yields a *Fokker–Planck* (FP) equation describing the evolution of the probability density of a corresponding continuous stochastic process that is the solution to a *stochastic differential equation* (SDE), which in the physics literature is often called a *Langevin equation*; we will take these terms to be interchangeable. Further details concerning SDEs can be found in appendix section 1.7 and in various references [210, 476]. Moreover, a rigorous analysis of the diffusion approximation and its relationship to the system-size expansion has been carried out by Kurtz [352].

First, introduce the rescaled variable $x = n/N$ and transition rates $N\Omega_\pm(x) = \omega_\pm(Nx)$. Equation (1.104) can then be rewritten in the form

$$\frac{dp(x,t)}{dt} = N[\Omega_+(x-1/N)p(x-1/N,t) + \Omega_-(x+1/N)p(x+1/N,t) \\ -(\Omega_+(x) + \Omega_-(x))p(x,t)].$$

Treating $x, 0 \le x \le 1$, as a continuous variable and Taylor expanding terms on the right-hand side to second order in N^{-1} leads to the FP equation

$$\frac{\partial p(x,t)}{\partial t} = -\frac{\partial}{\partial x}[A(x)p(x,t)] + \frac{1}{2N}\frac{\partial^2}{\partial x^2}[B(x)p(x,t)] \qquad (1.111)$$

with

$$A(x) = \Omega_+(x) - \Omega_-(x) \equiv \alpha - (\alpha + \beta)x, \qquad (1.112a)$$
$$B(x) = \Omega_+(x) + \Omega_-(x) \equiv \alpha + (\beta - \alpha)x. \qquad (1.112b)$$

The FP equation takes the form of a conservation equation

$$\frac{\partial p}{\partial t} = -\frac{\partial J}{\partial x}, \qquad (1.113)$$

where $J(x,t)$ is the probability flux,

$$J(x,t) = -\frac{1}{2N}\frac{\partial}{\partial x}[B(x)p(x,t)] + A(x)p(x,t). \qquad (1.114)$$

The FP equation is supplemented by the no-flux or reflecting boundary conditions at the ends $x = 0, 1$ and a normalization condition,

$$J(0,t) = J(1,t) = 0, \quad \int_0^1 p(x,t)dx = 1. \qquad (1.115)$$

The FP equation has a unique steady-state solution obtained by setting $J(x,t) = 0$ for all $0 \le x \le 1$. The resulting first-order ODE can be solved to give a steady-state probability density of the form (1.107), with corresponding potential

$$\Phi_{FP}(x) = -2\int^x \frac{A(x')}{B(x')}dx' = -2\int^x \frac{\Omega_+(x') - \Omega_-(x')}{\Omega_+(x') + \Omega_-(x')}dx'. \qquad (1.116)$$

The mean and variance of the fraction of open channels close to the fixed point x^* can again be determined by carrying out a Gaussian approximation, and the results agree with those obtained from the steady-state solution of the master equation. An alternative way of calculating the mean and variance is to note that the solution to the FP equation (1.111) determines the probability density function for a corresponding stochastic process $X(t)$, which evolves according to the SDE or Langevin equation [210]

$$dX = A(X)dt + \frac{1}{\sqrt{N}}b(X)dW(t). \tag{1.117}$$

with $b(x)^2 = B(x)$. Here $W(t)$ denotes a Wiener process with $dW(t)$ distributed according to a Gaussian process with mean and covariance

$$\langle dW(t) \rangle = 0, \quad \langle dW(t)dW(s) \rangle = \delta(t-s)dtds. \tag{1.118}$$

Note that the noise term in (1.117) is multiplicative, since it depends on the current state $X(t)$. It is well known that there is an ambiguity in how one integrates multiplicative noise terms, which relates to the issue of Ito versus Stratonovich versions of stochastic calculus [210]; see appendix section1.7. However, for this particular example, based on the reduction of a master equation, the explicit form of the corresponding FP equation (1.111) ensures that the noise should be interpreted in the sense of Ito.

Thus, one can view the SDE as describing a stochastic path in phase space that involves a deterministic trajectory converging to the unique stable fixed point x^* that is perturbed by Gaussian-like fluctuations of order $1/\sqrt{N}$. Substituting $X - x^* = Y/\sqrt{N}$ into the SDE equation (1.117) and formally Taylor expanding to lowest order in $1/\sqrt{N}$ yields the so-called linear noise approximation

$$dY = -kYdt + b(x^*)dW(t), \tag{1.119}$$

with

$$k \equiv -A'(x^*) = \alpha + \beta, \quad b(x^*) = \sqrt{B(x^*)} = \sqrt{\frac{2\alpha\beta}{\alpha+\beta}}.$$

This takes the form of an Ornstein–Uhlenbeck equation [210], which can be solved as

$$Y(t) = e^{-kt}Y_0 + b(x^*)\int_0^t e^{-k(t-t')}dW(t'), \tag{1.120}$$

given the initial condition $Y(0) = Y_0$. It follows that the mean and covariance of $Y(t)$ are

$$\langle Y(t) \rangle = e^{-kt}Y_0, \tag{1.121}$$

and

$$\text{cov}(Y(t), Y(s)) \equiv \langle [Y(t) - \langle Y(t) \rangle][Y(s) - \langle Y(s) \rangle] \rangle \tag{1.122}$$

$$= \left\langle b(x^*)^2 \left[\int_0^t e^{-k(t-t')}dW(t')\right]\left[\int_0^s e^{-k(s-t'')}dW(t'')\right]\right\rangle$$

$$= b(x^*)^2 e^{-k(t+s)}\int_0^s e^{2kt'}dt' = \frac{b(x^*)^2}{2k}e^{-k(t-s)}\left[1 - e^{-2ks}\right].$$

Here

$$\frac{b(x^*)^2}{2k} = \frac{\alpha\beta}{(\alpha+\beta)^2} = x^*(1-x^*),$$

and, without loss of generality, we have assumed that $t \geq s$. Thus, in the stationary limit $t \to \infty$,

$$\langle Y(t) \rangle \to 0, \quad \text{cov}(Y(t), Y(s)) \to \frac{b(x^*)^2}{2k} e^{-k|t-s|}.$$

Since $Y(t)/\sqrt{N} = X(t) - x^*$, we recover the results of (1.110).

Note that (1.116) differs from the effective potential (1.107) obtained directly from the master equation for large N, given that the latter can be rewritten in the form

$$\Phi(x) = \int^x \ln \frac{\Omega_-(x')}{\Omega_+(x')} dx'. \tag{1.123}$$

Although, this discrepancy is not much of an issue when the underlying kinetic equations have a unique fixed point, it can lead to exponentially large errors when there are multiple stable fixed points. The Langevin or diffusion approximation still accounts for the effects of fluctuations well within the basin of attraction of a locally stable fixed point. However, there is now a small probability that there is a noise-induced transition to the basin of attraction of another fixed point. Since the probability of such a transition is usually of order $e^{-\tau N}$ with $\tau = \mathcal{O}(1)$, except close to the boundary of the basin of attraction, such a contribution cannot be analyzed accurately using standard Fokker–Planck methods [309]. These exponentially small transitions play a crucial role in allowing the network to approach the unique stationary state (if it exists) in the asymptotic limit $t \to \infty$. In other words, for multistable systems, the limits $t \to \infty$ and $N \to \infty$ do not commute [24, 256, 641]. One example where multistability is important is when considering the effects of stochastic ion channels on membrane voltage fluctuations (see below).

1.5.3 Membrane Voltage Fluctuations

Let us now return to a conductance-based model of a neuron, in which the stochastic opening of ion channels generates a stochastic ionic current that drives the membrane voltage. We are particularly interested in how fluctuations affect the initiation of an action potential due to the opening of a finite number of Na^+ channels. Therefore, we imagine freezing the slow K^+ channels, so that they effectively act as a leak current and simplify the sodium channels by treating each as a single activating subunit. The stochastic membrane voltage then evolves according to the piecewise deterministic equation

$$\frac{dV}{dt} = F(V, n) \equiv \frac{1}{N} f(V) n(t) - g(V), \tag{1.124}$$

where $f(v) = g_{Na}(V_{Na} - v)$ represents the gated sodium currents, $g(v) = -g_{eff}[V_{eff} - v] - I$ represents the sum of effective leakage currents and external inputs I, and $n(t)$ is the number of open sodium channels. Note that (1.124) only holds between jumps in the number of open ion channels, with the latter described by the

master equation (1.104). The stochastic process defined by (1.104) and (1.124) is an example of a so-called stochastic hybrid system with piecewise deterministic dynamics. There has been a lot of recent interest in such systems, particularly within the context of conductance-based models [88, 321, 484, 654]. The associated probability density $p(v,n,t)$, which is defined according to

$$p(v,n,t)dv = \text{Prob}[n(t) = n, v \leq V(t) \leq v + dv],$$

given an initial condition $V(0) = V_0, n(0) = n_0$, satisfies the differential Chapman–Kolmogorov (CK) equation

$$\frac{\partial p}{\partial t} = -\frac{\partial}{\partial v}\left[\left(\frac{n}{N}f(v) - g(v)\right)p\right] + \omega_+(v,n-1)p(v,n-1,t) \qquad (1.125)$$
$$+ \omega_-(v,n+1)p(v,n+1,t) - [\omega_+(v,n) + \omega_-(v,n)]p(v,n,t),$$

with

$$\omega_+(v,n) = \alpha(v)(N-n), \quad \omega_-(v,n) = \beta(v)n. \qquad (1.126)$$

Note that the right-hand side of (1.124) is negative for large V and positive for small V, which implies that the voltage V is confined to some bounded domain $[V_1, V_2]$.

In order to investigate action potential initiation, we will assume that N is sufficiently large so that we can approximate the jump Markov process for the ion channels by a continuous Markov process using a diffusion approximation, and (ii) we assume that the transitions between different discrete states is much faster than the voltage dynamics so we can assume that, for fixed v, the number of open ion channels is close to the quasi-equilibrium $x^*(v) = \alpha(v)/(\alpha(v) + \beta(v))$. This limiting case was originally considered by Chow and White [116]. Under these approximations, the voltage dynamics is described by an SDE of the form [see (1.119)]

$$dV = \left[f(V)(x^* + Y(t)/\sqrt{N}) - g(V)\right]dt, \quad dY = -kYdt + b(x^*)dW(t). \quad (1.127)$$

Thus the stochastic voltage is coupled to a fast Ornstein–Uhlenbeck or colored noise process $Y(t)$. If we make the further assumption that the latter is in quasi-equilibrium for a given V (fast ion channels), $Y(t)dt \approx k^{-1}b(x^*)dW(t)$, then we obtain a scalar SDE for the voltage:

$$dV = [f(V)x^*(V) - g(V)]dt + \frac{1}{\sqrt{N}}\sigma(V)f(V)dW(t), \qquad (1.128)$$

where

$$\sigma(V) = \frac{b(x^*(V))}{k(V)} = \frac{1}{\alpha(V) + \beta(V)}\sqrt{\frac{2\alpha(V)\beta(V)}{\alpha(V) + \beta(V)}}. \qquad (1.129)$$

Taking $\alpha, \beta = \mathcal{O}(1/\varepsilon)$ for some dimensionless parameter $0 < \varepsilon \ll 1$, we see that $\sigma(V) = \mathcal{O}(\varepsilon^{1/2})$. In deriving (1.128), we have effectively taken a zero correlation limit of a colored noise process. It can be shown that the multiplicative noise term should be interpreted in the sense of Stratonovich, and the associated FP equation is given by [210, 321]

$$\frac{\partial p(v,t)}{\partial t} = -\frac{\partial}{\partial v}[\mathscr{A}(v)p(v,t)] + \frac{1}{N}\frac{\partial}{\partial v}\left[\mathscr{B}(v)\frac{\partial}{\partial v}p(v,t)\right], \qquad (1.130)$$

with

$$\mathscr{A}(v) = f(v)x^*(v) - g(v), \quad \mathscr{B}(v) = [\sigma(v)f(v)]^2/2.$$

We have ignored an $\mathcal{O}(\varepsilon)$ contribution to the drift term of the form $\mathscr{B}'(v)/N$. The FP equation is supplemented by reflecting boundary conditions at $v = V_1, V_2$:

$$J(V_1,t) = J(V_2,t) = 0, \qquad (1.131)$$

with

$$J(v,t) = \mathscr{A}(v)p(v,t) - \frac{\mathscr{B}(v)}{N}\frac{\partial}{\partial v}p(v,t). \qquad (1.132)$$

1.5.4 First Passage Time Problem

A key property that one would like to calculate is the mean time to fire an action potential (MFPT) as a function of the stimulus current I. In the absence of noise, the system evolves according to the deterministic equation

$$\frac{dv}{dt} = \mathscr{A}(v) = \frac{\alpha(v)}{\alpha(v) + \beta(v)}f(v) - g(v) \equiv -\frac{d\Phi_0(v)}{dv}, \qquad (1.133)$$

where $\Phi_0(v)$ is a deterministic potential. In Fig. 1.17, we plot $\Phi_0(v)$ as a function of v for various values of the external input current and the particular transition rates

$$\alpha(v) = \beta \exp\left(\frac{2(v - v_1)}{v_2}\right), \quad \beta = \text{constant}.$$

The minima and maxima of the potential correspond to stable and unstable fixed points of the deterministic dynamics, respectively. It can be seen that below a threshold current I_*, $I < I_*$, there exist two stable fixed points $v_\pm$ (minima) separated by an unstable fixed point at v_0 (maximum), that is, the system exhibits bistability. The left-hand fixed point represents the resting state, whereas the right-hand fixed point corresponds to an excited state. Thus, in the bistable regime the deterministic system requires an external perturbation in order to generate an action potential starting from the resting state. On the other hand, for the stochastic system it is possible that fluctuations in the opening and closing of Na^+ ion channels induce a transition from the resting state to the excited state by crossing over the potential hill at v_0. This is directly analogous to a diffusing particle escaping from the left to the right well in a double well potential, which is a classical example of a first passage time (FPT) problem in physics [210, 257]. (Of course, once such an event occurs, one has to take into account the K^+ dynamics in order to incorporate the effects of repolarization

that return the system to the resting state. If one includes the slow opening and closing of these channels, then the underlying deterministic system becomes excitable rather than bistable; see Sect. 2.1. For the moment, we will assume that this does not significantly affect the noise-induced initiation of an action potential. It turns out that such an assumption breaks down if fluctuations in the opening and closing of K^+ channels become significant [456].)

We now outline the basic calculation of the mean time to escape from the resting state using the diffusion approximation. Since the voltage will rapidly approach the excited state v_+ once it has passed the maximum at v_0, the major contribution to the escape time will be due to the fluctuation-driven transition from v_- to v_0. We can model this process by replacing the reflecting boundary condition at $v = V_2$ with an absorbing boundary condition at $v = v_0 < V_2$:

$$p(v_0,t) = 0.$$
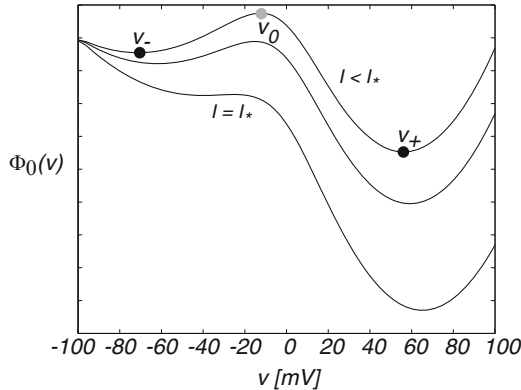
Fig. 1.17 Plot of deterministic potential $\Phi_0(v)$ as a function of voltage v for different values of the external stimulus current I. Parameter values are $N = 10$, $v_{Na} = 120$ mV, $v_{eff} = -62.3$ mV, $g_{Na} = 4.4$ mS/cm^2, $g_{eff} = 2.2$ mS/cm^2, $\beta = 0.8$ s^{-1}, and $\alpha(v) = \beta \exp[(v+1.2)/9]$

We also shift the voltage v so that the left-hand boundary is at $V_1 = 0$. Let $T(v)$ denote the stochastic time for the particle to exit the right-hand boundary at v_0, given that it starts at location $v \in [0, v_0]$ at time $t = 0$. As a first step, we introduce the survival probability $\mathbb{P}(v,t)$ that the particle has not yet exited at time t:

$$\mathbb{P}(v,t) = \int_0^{v_0} p(x,t|v,0)dx. \tag{1.134}$$

It follows that $\text{Prob}[T(v) \leq t] = 1 - \mathbb{P}(v,t)$ and we can define the FPT density according to

$$f(v,t) = -\frac{\partial \mathbb{P}(v,t)}{\partial t}. \tag{1.135}$$

It can be shown from (1.130) and the Markovian nature of the stochastic process that the FPT density satisfies a backward FP equation of the form [210]

$$\frac{\partial \mathbb{P}(v,t)}{\partial t} = \mathscr{A}(v)\frac{\partial \mathbb{P}(v,t)}{\partial v} + \frac{\partial}{\partial v}\left(\mathscr{B}(v)\frac{\partial}{\partial v}\mathbb{P}(v,t)\right), \qquad (1.136)$$

where we have absorbed the factor of $1/N$ into $\mathscr{B}$.

A quantity of particular interest is the mean first passage time (MFPT) $\tau(v)$ defined according to

$$\tau(v) = \langle T(v) \rangle \equiv \int_0^\infty f(v,t)t\,dt \qquad (1.137)$$
$$= -\int_0^\infty t\frac{\partial \mathbb{P}(v,t)}{\partial t}dt = \int_0^\infty \mathbb{P}(v,t)dt,$$

after integration by parts. Hence, integrating both sides of (1.136) shows that the MFPT satisfies the ODE

$$[\mathscr{A}(v)+\mathscr{B}'(v)]\frac{d\tau(v)}{dv} + \left(\mathscr{B}(v)\frac{d^2}{dv^2}\tau(v)\right) = -1. \qquad (1.138)$$

Equation (1.138) is supplemented by reflecting and absorbing boundary conditions for the backward FP equation:

$$\tau'(0) = 0, \quad \tau(v_0) = 0. \qquad (1.139)$$

It is straightforward to solve (1.138) by direct integration [210]. First, introducing an integration factor and integrating once gives

$$e^{\Psi(v)}\tau'(v) = -\int_0^v \frac{e^{\Psi(v')}}{\mathscr{B}(v')}dv',$$

where

$$\Psi(v) = \int_0^v \frac{\mathscr{A}(v')+\mathscr{B}'(v')}{\mathscr{B}(v')}dv'. \qquad (1.140)$$

and we have used the boundary condition $\tau'(0) = 0$. Integrating once more with respect to v and using $\tau(v_0) = 0$ then gives

$$\tau(v) = \int_v^{v_0} e^{-\Psi(v')}dv'\int_0^{v'} \frac{e^{\Psi(v'')}}{\mathscr{B}(v'')}dv''. \qquad (1.141)$$

There is now a standard procedure for approximating this double integral based on Kramers reaction rate theory [210, 257]. We simply quote the result here: $\tau(v_-) = 1/\lambda$ where

$$\lambda \approx \frac{\mathscr{B}(v_0)}{\pi}\sqrt{\left|\frac{\mathscr{A}'(v_-)}{\mathscr{B}(v_-)}\right|\frac{\mathscr{A}'(v_0)}{\mathscr{B}(v_0)}}\exp\left[\int_{v_-}^{v_0}\frac{\mathscr{A}(v)}{\mathscr{B}(v)}dv\right]. \qquad (1.142)$$
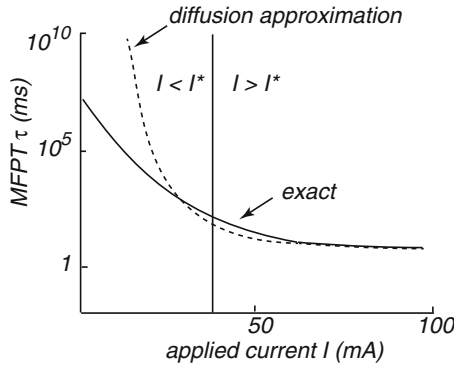
Fig. 1.18 Schematic diagram comparing MFPT calculated using the diffusion approximation with the MFPT of the full system. The scales of the axes are based on numerical results carried out in [321] for $N = 10$. Other parameter values as in Fig. 1.17

Keener and Newby [321] calculated the MFPT using the diffusion approximation and compared it with Monte Carlo simulations of the full stochastic model whose probability density evolves according to the CK equation (1.126). A summary of their findings is shown schematically in Fig. 1.18. The main observation is that although the Gaussian-like diffusion approximation does well in the superthreshold regime ($I > I_*$), it deviates significantly from the full model results in the subthreshold regime ($I < I_*$), where it overestimates the mean time to spike. This is related to the fact that the effective potential of the steady-state density under the diffusion approximation generates exponentially large errors in the MFPT, as discussed at the end of Sect. 1.5.2. Finally, note that the model of stochastic ion channels and membrane voltage fluctuations presented above is based on a number of simplifications. First, only the initiation of an action potential was considered, which involved the opening of sodium channels, while the termination of the action potential due to Na^+ inactivation and K^+ activation was ignored. Indeed, in stochastic versions of the Hodgkin–Huxley equations spontaneous activity can be observed due to fluctuations in K^+ ion channels [116, 456]. That is, if some K^+ channels spontaneously close, then a regenerative Na^+ current can induce an action potential. The second simplification was to treat each ion channel as a single unit rather than as a cluster of subunits. In other words, the Markov chain of events associated with opening and closing of an ion channel involves transitions between more than two internal states.

1.6 Stochastic Hybrid System with Fast Kinetics

As shown by Keener and Newby [321], it is possible to obtain a much more accurate analytical expression for the MFPT in the subthreshold regime by analyzing the CK equation (1.126) in the limit of fast sodium channels. This analysis applies equally

well to small and large N. First, it is convenient to rewrite the CK equation in a more compact and general form:

$$\frac{\partial p}{\partial t} = -\frac{\partial [F(v,n)p(v,n,t)]}{\partial v} + \frac{1}{\varepsilon} \sum_{m=0}^{N} A(n,m;v)p(v,m,t) \qquad (1.143)$$

with F given by (1.124) and A a tridiagonal matrix (for fixed v): $A(n,n-1;v) = \omega_+(v,n-1)$, $A(n,n;v) = -\omega_+(v,n) - \omega_-(n)$, $A(n,n+1;v) = \omega_-(n+1)$. We are now making explicit the condition that the open and closing of Na$^+$ channels occurs on a much faster time scale than the voltage dynamics by scaling the transition rates according to the small parameter $\varepsilon \ll 1$. In the limit $\varepsilon \to 0$, (1.124) reduces to the deterministic or mean field (1.133) with $\mathscr{A}(v) = \sum_n F(v,n)\rho(v,n)$, where $\rho(v,n)$ is the unique steady-state density satisfying $\sum_m A(n,m;v)\rho(v,m) = 0$ (see (1.105)):

$$\rho(v,n) = \frac{N!}{(N-n)!n!}a(v)^n b(v)^{N-n}, \quad a(v) = \frac{\alpha(v)}{\alpha(v)+\beta}, b(v) = \frac{\beta}{\alpha(v)+\beta}. \quad (1.144)$$

The mean number of open channels is $\langle n \rangle = \sum_{n=1}^{N} n\rho(v,n) = Na(v)$. In the regime $0 < \varepsilon \ll 1$, for which there are typically a large number of transitions between different channel states n while the voltage v hardly changes at all. This suggests that the system rapidly converges to the (quasi-)steady-state $\rho(v,n)$, which will then be perturbed as v slowly evolves. The resulting perturbations can be analyzed using a quasi-steady-state (QSS) diffusion or adiabatic approximation [210, 454, 487], in which the CK equation (1.143) is approximated by a Fokker–Planck (FP) equation; see also Sect. 6.4

The QSS approximation was first developed from a probabilistic perspective by Papanicolaou [487]; see also [210]. It has subsequently been applied to a wide range of problems in biology, including cell movement [274, 481], wavelike behavior in models of slow axonal transport [206, 207, 518], and molecular motor-based models of random intermittent search [453, 454]. The basic idea of the QSS reduction is to decompose the probability density as

$$p(v,n,t) = C(v,t)\rho(v,n) + \varepsilon w(v,n,t), \qquad (1.145)$$

where $\sum_n p(v,n,t) = C(v,t)$ and $\sum_n w(v,n,t) = 0$. Carrying out an asymptotic expansion in ε, it can be shown that C evolves according to the FP equation [81, 453, 454]

$$\frac{\partial C}{\partial t} = -\frac{\partial}{\partial v}(\mathscr{A}C) + \varepsilon\frac{\partial}{\partial v}\left(\mathscr{D}\frac{\partial C}{\partial v}\right), \qquad (1.146)$$

with the drift term given by (1.133), and diffusion coefficient

$$\mathscr{D}(v) = \sum_{n=0}^{N} Z(v,n)F(v,n), \qquad (1.147)$$

where $Z(v,n)$ is the unique solution to

$$\sum_m A(n,m;v)Z(v,m) = [\mathscr{A}(v) - F(v,n)]\rho(v,n) \tag{1.148}$$

with $\sum_m Z(v,m) = 0$. As in the case of the diffusion approximation for large N, the FP equation (1.146) captures the Gaussian-like fluctuations within the basin of attraction of a fixed point of the mean field (1.133), but breaks down when considering rare event transitions between metastable states since it yields exponentially large errors in the escape rates. Therefore, one has to deal with the full CK equation (1.143).

1.6.1 First Passage Time Problem and the Projection Method

In order to revisit the FPT problem considered in Sect. 1.5.4, we supplement (1.143) with the following absorbing boundary conditions at v_0:

$$p(v_0,n,t) = 0, \text{ for all } n \in \Sigma = \{0,\ldots,k-1\}. \tag{1.149}$$

Here, Σ denotes the set of integers for which $F(v_0,n) < 0$. The initial condition is taken to be

$$p(v,n,0) = \delta(v - v_-)\delta_{n,n_0}. \tag{1.150}$$

Let T denote the (stochastic) FPT for which the system first reaches v_0, given that it started at v_-. The distribution of FPTs is related to the survival probability that the system has not yet reached v_0:

$$S(t) \equiv \int_0^{v_0} \sum_{n=0}^N p(v,n,t)dv. \tag{1.151}$$

That is, $\text{Prob}\{t > T\} = S(t)$ and the FPT density is

$$f(t) = -\frac{dS}{dt} = -\int_0^{v_0} \sum_{n=0}^N \frac{\partial p}{\partial t}(v,n,t)dv. \tag{1.152}$$

Substituting for $\partial p/\partial t$ using the CK equation (1.143) shows that

$$f(t) = \int_0^{v_0} \left[\sum_{n=0}^N \frac{\partial [F(v,n)p(v,n,t)]}{\partial v} \right] dv = \sum_{n=0}^N p(v_0,n,t)F(v_0,n). \tag{1.153}$$

We have used $\sum_n A(n,m;v) = 0$ and $\lim_{v \to -\infty} F(v,n)p(v,n,t) = 0$. The FPT density can thus be interpreted as the probability flux $J(v,t)$ at the absorbing boundary, since we have the conservation law

$$\sum_{n=0}^N \frac{\partial p(v,n,t)}{\partial t} = -\frac{\partial J(v,t)}{\partial v}, \quad J(v,t) = \sum_{n=0}^N F(v,n)p(v,n,t). \tag{1.154}$$

We wish to solve the FPT problem in the weak noise limit $\varepsilon \ll 1$. One of the characteristic features of the weak noise limit is that the flux through the absorbing boundary and the inverse of the MFPT $\langle T \rangle$ are exponentially small, that is, $\langle T \rangle \sim e^{-C/\varepsilon}$ for some constant C. This means that standard singular perturbation theory cannot be used to solve the resulting boundary value problem, in which one matches inner and outer solutions of a boundary layer around the point $v = v_0$. Instead, one proceeds by finding a quasistationary solution using a Wentzel–Kramers–Brillouin (WKB) approximation. Recently, this approach has been extended by Keener and Newby [321] to a CK equation of the form (1.143), using a so-called projection method [660].

In order to apply the projection method, it is necessary to assume certain properties of the non-self-adjoint linear operator $-\hat{L}$ on the right-hand side of (1.143) with respect to the Hilbert space of functions $h : [0, v_0] \times \{0, \ldots, N\} \to \mathbb{R}$ with inner product defined according to

$$\langle h, g \rangle = \int_0^{v_0} \sum_{n=0}^N h(v, n) g(v, n) dv. \tag{1.155}$$

1. $\hat{L}$ has a complete set of eigenfunctions ϕ_r with

$$\hat{L}\phi_r(v, n) \equiv \frac{d}{dv}(F(v, n)\phi_r(v, n)) - \frac{1}{\varepsilon} \sum_{m=0}^N A(n, m; v)\phi_r(v, m) = \lambda_r \phi_r(v, n), \tag{1.156}$$

   together with the boundary conditions

$$\phi_r(v_0, n) = 0, \text{ for } n = 0, \ldots, k-1. \tag{1.157}$$

2. The real part of each eigenvalue λ_r is positive definite and the smallest eigenvalue λ_0 is real and simple. Thus we can introduce the ordering $0 < \lambda_0 < \text{Re}[\lambda_1] \leq \text{Re}[\lambda_2] \leq \ldots$.
3. λ_0 is exponentially small, $\lambda_0 \sim e^{-C/\varepsilon}$, whereas $\text{Re}[\lambda_r] = \mathcal{O}(1)$ for $r \geq 1$. In particular, $\lim_{\varepsilon \to 0} \lambda_0 = 0$ and $\lim_{\varepsilon \to 0} \phi_0(v, n) = \rho(v, n)$.

Under the above assumptions, we can introduce the eigenfunction expansion

$$p(v, n, t) = \sum_{r=0}^N C_r e^{-\lambda_r t} \phi_r(v, n), . \tag{1.158}$$

with $\lambda_0 \ll \text{Re}[\lambda_r]$ for all $r \geq 1$. Thus, at large times we have the quasistationary approximation

$$p(v, n, t) \sim C_0 e^{-\lambda_0 t} \phi_0(v, n). \tag{1.159}$$

Substituting such an approximation into (1.153) implies that

$$f(t) \sim e^{-\lambda_0 t} \sum_{n=0}^N \phi_0(v_0, n) F(v_0, n), \quad \lambda_1 t \gg 1. \tag{1.160}$$

Equation (1.156) implies that

$$\sum_{n=0}^{N}\int_0^{v_0}\widehat{L}\phi_0(v,n)dv \equiv \sum_{n=0}^{N}F(v_0,n)\phi_0(v_0,n)$$

$$= \lambda_0\sum_{n=0}^{N}\int_0^{v_0}\phi_0(v,n)dv.$$

In other words,

$$\lambda_0 = \frac{\sum_{n=0}^{N}F(v_0,n)\phi_0(v_0,n)}{\langle 1,\phi_0\rangle}. \tag{1.161}$$

Combining (1.161) and the quasistationary approximation (1.160) shows that the (normalized) FPT density reduces to

$$f(t) \sim \lambda_0 e^{-\lambda_0 t} \tag{1.162}$$

and, hence, $\langle T\rangle = \int_0^\infty t f(t)dt \sim 1/\lambda_0$.

It remains to obtain an approximation ϕ_ε of the principal eigenfunction ϕ_0, which can be achieved using the WKB method as described in Sect. 1.6.2. This yields a quasistationary density that approximates ϕ_0 up to exponentially small terms at the boundary, that is,

$$\hat{L}\phi_\varepsilon = 0, \quad \phi_\varepsilon(u_*,n) = \mathcal{O}(e^{-C/\varepsilon}). \tag{1.163}$$

In order to express λ_0 in terms of the quasistationary density ϕ_ε, we consider the eigenfunctions of the adjoint operator, which satisfy the equation

$$\hat{L}^\dagger\xi_r(v,n) \equiv -F(v,n)\frac{d\xi_r(v,n)}{dv} - \frac{1}{\varepsilon}\sum_m A(m,n;v)\xi_r(v,m) = \lambda_r\xi_r(v,n),$$
$$\tag{1.164}$$

and the boundary conditions

$$\xi_r(v_0,n) = 0, \quad n \geq k. \tag{1.165}$$

The two sets of eigenfunctions $\{\phi_r\}$ and $\{\xi_r\}$ form a biorthogonal set with respect to the underlying inner product,

$$\langle \phi_r,\xi_s\rangle = \delta_{r,s}. \tag{1.166}$$

Now consider the identity

$$\langle \phi_\varepsilon,\hat{L}^\dagger\xi_0\rangle = \lambda_0\langle \phi_\varepsilon,\xi_0\rangle. \tag{1.167}$$

Integrating by parts the left-hand side of (1.164) picks up a boundary term so that

$$\lambda_0 = -\frac{\sum_{n=0}^{N}\phi_\varepsilon(v_0,n)\xi_0(v_0,n)F(v_0,n)}{\langle \phi_\varepsilon,\xi_0\rangle}. \tag{1.168}$$

The calculation of the principal eigenvalue λ_0 thus reduces to the problem of determining the quasistationary density ϕ_ε and the adjoint eigenfunction ξ_0.

1.6.2 The WKB Method and the Quasistationary Density

We now show how the WKB method [160, 256, 398, 445, 559] can be used to compute the quasistationary density ϕ_ε. We seek a solution of the form

$$\phi_\varepsilon(v,n) \sim R(v,n)\exp\left(-\frac{\Phi(v)}{\varepsilon}\right), \qquad (1.169)$$

where $\Phi(v)$ is a scalar potential. Substituting into $\hat{L}\phi_\varepsilon = 0$ gives

$$\sum_{m=0}^{N} \left(A(n,m;v) + \Phi'(v)\delta_{n,m}F(v,m)\right)R(v,m) = \varepsilon\frac{dF(v,n)R(v,n)}{dx}, \quad (1.170)$$

where $\Phi' = d\Phi/dx$. Introducing the asymptotic expansions $R \sim R^{(0)} + \varepsilon R^{(1)}$ and $\Phi \sim \Phi_0 + \varepsilon\Phi_1$, the leading-order equation is

$$\sum_{m=0}^{N} A(n,m;v)R^{(0)}(v,m) = -\Phi_0'(v)F(v,n)R^{(0)}(v,n). \qquad (1.171)$$

(Note that since $F(v,n)$ is nonzero almost everywhere for $v < v_0$, we can identify $-\Phi_0'$ and $R^{(0)}$ as an eigenpair of the matrix operator $\hat{A}(n,m;v) = A(n,m;v)/F(v,n)$ for fixed v.) Positivity of the probability density ϕ_ε requires positivity of the corresponding solution $R^{(0)}$. One positive solution is $R^{(0)} = \rho$, for which $\Phi_0' = 0$. However, such a solution is not admissible since $\Phi_0 = $ constant. It can be proven using linear algebra that if $F(v,n)$ for fixed $v < v_0$ changes sign as n increases from zero, then there exists one other positive solution, which also has the appropriate functional form to describe the potential well. That is, $\Phi_0'(x)$ has the correct sign and vanishes at the fixed points. Hence, it can be identified as the appropriate WKB solution.

Proceeding to the next order in the asymptotic expansion of (1.170), we have

$$\sum_{m=0}^{N} \left(A(n,m;v) + \Phi_0'(v)\delta_{n,m}F(v,m)\right)R^{(1)}(v,m)$$

$$= \frac{dF(v,n)R^{(0)}(v,n)}{dx} - \Phi_1'(v)F(v,n)R^{(0)}(v,n). \qquad (1.172)$$

For fixed v and WKB potential Φ_0, the matrix operator $\bar{A}(n,m;v) = A(n,m;v) + \Phi_0'(v)\delta_{n,m}F(v,m)$ on the left-hand side of this equation has a one-dimensional null

space spanned by the positive WKB solution $R^{(0)}$. The Fredholm alternative theorem[1] then implies that the right-hand side of (1.172) is orthogonal to the left null vector S of $\bar{A}$. That is, we have the solvability condition

$$\sum_{n=0}^{N} S(v,n) \left[\frac{dF(v,n)R^{(0)}(v,n)}{dv} - \Phi_1'(v)F(v,n)R^{(0)}(v,n) \right] = 0, \qquad (1.173)$$

with S satisfying

$$\sum_{n=0}^{N} S(v,n) \left(A(n,m;v) + \Phi_0'(v)\delta_{n,m}F(v,m) \right) = 0. \qquad (1.174)$$

Given $R^{(0)}, S$ and Φ_0, the solvability condition yields the following equation for Φ_1:

$$\Phi_1'(x) = \frac{\sum_{n=0}^{N} S(v,n)[F(v,n)R^{(0)}(v,n)]'}{\sum_{n=0}^{N} S(v,n)F(v,n)R^{(0)}(v,n)}. \qquad (1.175)$$

Combining the various results, and defining

$$k(v) = \exp\left(-\int_{v_-}^{v} \Phi_1'(y)dy \right), \qquad (1.176)$$

gives to leading order in ε,

$$\phi_\varepsilon(v,n) \sim \mathcal{N}k(v)\exp\left(-\frac{\Phi_0(v)}{\varepsilon} \right) R^{(0)}(v,n), \qquad (1.177)$$

where we choose $\sum_n R^{(0)}(v,n) = 1$ for all v and $\mathcal{N}$ is the normalization factor,

$$\mathcal{N} = \left[\int_0^{v_0} k(v)\exp\left(-\frac{\Phi_0(v)}{\varepsilon} \right) \right]^{-1}. \qquad (1.178)$$

The latter can be approximated using Laplace's method to give

$$\mathcal{N} \sim \frac{1}{k(v_-)} \sqrt{\frac{|\Phi_0''(v_-)|}{2\pi\varepsilon}} \exp\left(\frac{\Phi_0(v_-)}{\varepsilon} \right). \qquad (1.179)$$

---

[1] Consider an M-dimensional linear inhomogeneous system $\mathbf{A}\mathbf{x} = \mathbf{b}$ with $\mathbf{x}, \mathbf{b} \in \mathbb{R}^M$. Suppose that the $M \times M$ matrix $\mathbf{A}$ has a nontrivial null space and let $\mathbf{v}$ be a null vector of the adjoint matrix $\mathbf{A}^\dagger$, that is, $\mathbf{A}^\dagger \mathbf{v} = 0$. The Fredholm alternative theorem states that the inhomogeneous equation has a (nonunique) solution if and only if $\mathbf{v} \cdot \mathbf{b} = 0$ for all null vectors $\mathbf{v}$.

1.6.3 Calculation of the Principal Eigenvalue

In order to evaluate the principal eigenvalue λ_0 satisfying (1.168), it is necessary to determine the adjoint eigenfunction ξ_0. Following [321, 455], this can be achieved using singular perturbation methods. Since λ_0 is exponentially small in ε, (1.164) yields the leading-order equation

$$\varepsilon F(v,n)\frac{d\xi_0(v,n)}{dx} + \sum_{m=0}^{N} A(m,n;v)\xi_0(v,m) = 0, \tag{1.180}$$

supplemented by the absorbing boundary condition

$$\xi_0(v_0,n) = 0, \quad n \geq k. \tag{1.181}$$

A first attempt at obtaining an approximate solution that also satisfies the boundary conditions is to construct a boundary layer in a neighborhood of the unstable fixed point v_0 by performing the change of variables $v = v_0 - \varepsilon z$ and setting $Q(z,n) = \xi_0(v_0 - \varepsilon z)$. Equation (1.180) then becomes

$$F(v_0,n)\frac{dQ(z,n)}{dz} + \sum_{m=0}^{N} A(m,n;v_0)Q(z,m) = 0. \tag{1.182}$$

This inner solution has to be matched with the outer solution $\xi_0 = \mathbf{1}$, which means that

$$\lim_{z\to\infty} Q(z,n) = 1 \tag{1.183}$$

for all n. Consider the eigenvalue equation

$$\sum_{n=0}^{N} (A(n,m;v) - \mu_r(v)\delta_{n,m}F(v,m))\, S_r(v,n) = 0, \tag{1.184}$$

with $r = 0,\ldots,N$. We take $S_0(v,n) = 1$ so that $\mu_0 = 0$ and set $S_1(v,n) = S(v,n), \mu_1(v) = -\Phi_0'(v)$, where S satisfies (1.174). We then introduce the eigenfunction expansion

$$Q(z,n) = c_0 + \sum_{r=1}^{N} c_r S_r(v_0,n)e^{-\mu_r(v_0)z}. \tag{1.185}$$

In order that the solution remains bounded as $z \to \infty$ we require that $c_r = 0$ if $\mathrm{Re}[\mu_r(v_0)] < 0$. The boundary conditions (1.181) generate a system of linear equations for the coefficients c_r with codimension k. One of the unknowns is determined by matching the outer solution, which suggests that there are $k-1$ eigenvalues with negative real part. The eigenvalues are ordered so that $\mathrm{Re}[\mu_r(v_0)] < 0$ for $r > N+1-k$.

There is, however, one problem with the above eigenfunction expansion, namely, that $\mu_1(v_0) \equiv -\Phi_0'(v_0) = 0$ so that the zero eigenvalue is degenerated at $v = v_0$. Hence, the solution needs to include a secular term involving the generalized eigen-

vector $\hat{S}$,

$$\sum_{n=0}^{N} A(n,m;v_0)\hat{S}(v_0,n) = -F(v_0,m). \qquad (1.186)$$

The Fredholm alternative theorem ensures that $\hat{S}$ exists and is unique, since the stationary density $\rho(v_0,m)$ is the right null vector of $A(n,m;v_0)$ and $\sum_n \rho(v_0,n)F(v_0,n) \equiv \mathscr{A}(v_0) = 0$; see (1.133). The solution for $\mathbf{Q}(z)$ is now

$$Q(z,n) = c_0 + c_1(\hat{S}(v_0,n) - z) + \sum_{r=2}^{N+1-k} c_r S_r(v_0,n)e^{-\mu_r(v_0)z}. \qquad (1.187)$$

The presence of the secular term means that the solution is unbounded in the limit $z \to \infty$, which means that the inner solution cannot be matched with the outer solution. One way to remedy this situation is to introduce an alternative scaling in the boundary layer of the form $v = v_0 + \varepsilon^{1/2}z$, as detailed in [455]. One can then eliminate the secular term $-c_1 z$ and show that

$$c_1 \sim \sqrt{\frac{2|\Phi_0''(v_0)|}{\pi}} + \mathscr{O}(\varepsilon^{1/2}), \quad c_r = \mathscr{O}(\varepsilon^{1/2}) \text{ for } r \geq 2 \qquad (1.188)$$

It turns out that we only require the first coefficient c_1 in order to evaluate the principal eigenvalue λ_0 using (1.168). This follows from (1.171) and (1.184) and the observation that the left and right eigenvectors of the matrix $\hat{A}(n,m;v) = A(n,m;v)/F(v,n)$ are biorthogonal. In particular, since the quasistationary approximation ϕ_ε is proportional to $R^{(0)}$ (see (1.177)), it follows that ϕ_ε is orthogonal to all eigenvectors S_r, $r \neq 1$. Simplifying the denominator of (1.168) by using the outer solution $\xi_0 \sim 1$, we obtain

$$\lambda_0 \sim -\frac{\sum_n \xi_0(v_0,n)F(v_0,n)\phi_\varepsilon(v_0,n)}{\langle \phi_\varepsilon, \mathbf{1} \rangle}$$

$$\sim c_1 \frac{k(v_0)B(v_0)}{k(v_-)} \sqrt{\frac{|\Phi''(v_-)|}{2\pi}} \exp\left(-\frac{\Phi_0(v_0) - \Phi_0(v_-)}{\varepsilon}\right), \qquad (1.189)$$

with

$$B(v_0) = -\sum_{n=0}^{\infty} \hat{S}(v_0,n)F(v_0,n)\rho(v_0,n). \qquad (1.190)$$

Substituting for c_1

$$\lambda_0 \sim \frac{1}{\pi}\frac{k(v_0)B(v_0)}{k(v_-)}\sqrt{\Phi_0''(v_-)|\Phi_0''(v_0)|}\exp\left(-\frac{\Phi_0(v_0) - \Phi_0(v_-)}{\varepsilon}\right). \qquad (1.191)$$

Finally, comparison of (1.186) and (1.190) with (1.148) and (1.147) establishes that $B(v_0) \equiv \mathscr{D}(v_0)$.

The above analysis holds for any CK equation of the form (1.143). There are essentially three basic steps needed in order to evaluate the escape rate formula (1.191), which we now apply to the specific model of membrane voltage fluctuations.

1. Find the unique nontrivial positive eigenfunction $\psi_n(v) = R^{(0)}(v,n)$ and associated eigenvalue $\mu(v) = -\Phi_0'(v)$. In the case of the stochastic ion-channel model, (1.171) takes the explicit form

$$(N-n+1)\alpha\psi_{n-1} - [n\beta + (N-n)\alpha]\psi_n + (n+1)\beta\psi_{n+1}$$
$$= \mu\left(\frac{n}{N}f(v) - g(v)\right)\psi_n \tag{1.192}$$

Motivated by the form of the stationary density $\rho(v,n)$, we try the solution

$$\psi_n(v) = \frac{\Lambda(v)^n}{(N-n)!n!}, \tag{1.193}$$

which yields the following equation relating Λ and μ:

$$\frac{n\alpha}{\Lambda} + \Lambda\beta(N-n) - n\beta - (N-n)\alpha = \mu\left(\frac{n}{N}f(v) - g(v)\right).$$

We now fix μ in terms of Λ so that the terms linear in n vanish:

$$\mu = \frac{N}{f}\left[\alpha\left(\frac{1}{\Lambda} + 1\right) - \beta(\Lambda + 1)\right].$$

Eliminating μ then shows that

$$\Lambda(v) = \frac{g(v)}{f(v) - g(v)}.$$

We deduce that

$$\mu(v) = N\frac{\alpha(v)f(v) - (\alpha(v)+\beta)g(v)}{g(v)(f(v) - g(v))}, \tag{1.194}$$

and the normalized eigenvector is

$$\psi_n(v) = \frac{N!}{(N-n)!n!}\frac{(f(v) - g(v))^{N-n}g(v)^n}{f(v)^N}. \tag{1.195}$$

Note that $\mu(v)$ vanishes at the fixed points v_-, v_0 of the mean field (1.133) with $\mu(v) > 0$ for $0 < v < v_-$ and $\mu(v) > 0$ for $v_- < v < v_0$. Moreover, $\psi_n(v) = \rho(v,n)$ at the fixed points $v_0, v_\pm$. In conclusion $R^{(0)}(v,n) = \psi_n(v)$ and the effective potential Φ_0 is given by

$$\Phi_0(v) = -\int_{v_-}^v \mu(y)dy. \tag{1.196}$$

The effective potential is defined up to an arbitrary constant, which has been fixed by setting $\Phi_0(v_-) = 0$.

2. Determine the null eigenfunction $\eta_n(v) = S(v,n)$ of (1.174), which becomes

$$(N-m)\alpha\eta_{m+1} - [(N-m)\alpha + m\beta]\eta_m + m\beta\eta_{m-1}$$
$$= \mu\left(\frac{m}{N}f(v) - g(v)\right)\eta_m. \tag{1.197}$$

Trying a solution of the form $\eta_m(v) = \Gamma(v)^m$ yields

$$(N-m)\alpha\Gamma - ((N-m)\alpha + m\beta) + m\beta\Gamma^{-1} = \mu\left(\frac{m}{N}f(v) - g(v)\right). \tag{1.198}$$

Γ is then determined by canceling terms independent of m, which gives

$$\eta_n(v) = \left(\frac{b(v)g(v)}{a(v)(f(v)-g(v)))}\right)^n. \tag{1.199}$$

The prefactor $k(v)$ may now be determined using (1.175) and (1.176).

3. Calculate the generalized eigenvector $\zeta_n = \hat{S}(v_0,n)$ of (1.186), which reduces to

$$(N-n)\alpha(v_0)\zeta_{n+1} + n\beta\zeta_{n-1} - ((N-n)\alpha(v_0) + n\beta)\zeta_n = g(v_0) - \frac{n}{N}f(v_0). \tag{1.200}$$

It is straightforward to show that this has the solution

$$\zeta_n = \frac{f(v_0)}{N(\alpha(v_0) + \beta)}n. \tag{1.201}$$

It follows that the factor $B(v_0)$ defined by (1.190) is

$$\begin{aligned}
B(v_0) &= -\frac{f(v_0)}{N(\alpha(v_0) + \beta)}\sum_{n=0}^{N}\rho(v_0,n)\left[-g(v_0)n + \frac{f(v_0)}{N}n^2\right] \\
&= -\frac{f(v_0)}{N(\alpha(v_0) + \beta)}\left[-g(v_0)\langle n\rangle + \frac{f(v_0)}{N}\langle n^2\rangle\right] \\
&= \frac{f(v_0)^2\alpha(v_0)\beta}{N(\alpha(v_0) + \beta)^3}, \tag{1.202}
\end{aligned}$$

where have used the fixed point condition $g(v_0) = f(v_0)a(v_0)$.

Keener and Newby [321] showed that the WKB and asymptotic methods outlined above yield a MFPT that was in excellent agreement with numerical simulations in both the superthreshold and subthreshold regimes.

1.7 Appendix: Stochastic Calculus

In this appendix we give an informal introduction to stochastic calculus, following along the lines of Jacobs [302]. A more detailed treatment can be found in Gardiner [210], and a rigorous mathematical account can be found in [476]. The basic approach is to treat a continuous-time stochastic process as the limit of a discrete time process. That is, an SDE prescribes how a stochastic variable $X(t)$ changes in each infinitesimal time step dt. Determining changes over finite times then requires evaluating an associated stochastic integral. In order to make sense of this, we discretize time into small, but finite, intervals of duration Δt and consider a corresponding stochastic difference equation for $X_n = X(n\Delta t)$.

1.7.1 Ito Calculus

Suppose that we divide the time interval $[0,T]$ into N increments of size $\Delta t = T/N$ and set $t_n = n\Delta t$. Consider the stochastic difference equation

$$\Delta X(t_n) \equiv X(t_{n+1}) - X(t_n) = \Delta W_n,$$

where each ΔW_n, $n = 0, \ldots, N-1$, is an independent, identically distributed (i.i.d) Gaussian variable with zero mean and variance $\sigma^2 = \Delta t$:

$$P(\Delta W) = \frac{1}{\sqrt{2\pi\Delta t}} e^{-(\Delta W)^2/2\Delta t}. \tag{1.203}$$

Iterating the difference equation starting from $X(0) = 0$ yields

$$X_n \equiv X(n\Delta t) = \sum_{j=0}^{n-1} \Delta W_j.$$

Using the fact that the sum of Gaussian random variables is also a Gaussian, it follows that the probability density for X_n is a Gaussian. Thus, we only need to determine its mean and variance. Since the ΔW_j are all independent, we have

$$\langle X_n \rangle = \sum_{j=0}^{n-1} \langle \Delta W_j \rangle = 0, \quad \mathrm{Var}(X_n) = \sum_{j=0}^{n-1} \mathrm{Var}(\Delta W_j) = N\Delta t,$$

and

$$P(X_n) = \frac{1}{\sqrt{2\pi n\Delta t}} e^{-X_n^2/(2n\Delta t)}.$$

We can now construct a corresponding continuous-time process by taking the limit $N \to \infty$ such that $\Delta t \to 0$ with $N\Delta T = T$ fixed. In particular,

$$X(T) = \lim_{N\to\infty} \sum_{j=0}^{N-1} \Delta W_j \equiv \int_0^T dW(t) \equiv W(T),$$

where $W(T)$ is identified as a Wiener process. (A rigorous treatment would be more precise with regard to what is meant by the convergence of random variables.) It is still a Gaussian, whose mean and variance are obtained by taking the limit $N \to \infty$ of the results for X_n. We deduce that $W(t)$ has the Gaussian probability density

$$P(w(t)) = \frac{1}{\sqrt{2\pi t}} e^{-w(t)^2/2t}.$$

Now consider the modified stochastic difference equation

$$X_{n+1} - X_n = f(t_n)\Delta W_n,$$

where $f(t)$ is a deterministic function of time. Once again X_n is a Gaussian random variable, with

$$\langle X_n \rangle = \sum_{j=0}^{n-1} \langle f(t_j)\Delta W_j \rangle = 0, \quad \mathrm{Var}(X_n) = \sum_{j=0}^{n-1} \mathrm{Var}(f(t_j)\Delta W_j) = \sum_{j=0}^{n-1} f(t_j)^2 \Delta t.$$

Taking the continuum limit along identical lines to the previous case yields the continuous-time Gaussian variable

$$X(T) = \lim_{N \to \infty} \sum_{j=0}^{N-1} f(t_j)\Delta W_j \equiv \int_0^T f(t)dW(t), \tag{1.204}$$

with zero mean and variance

$$\mathrm{Var}(X(T)) = \int_0^T f(s)^2 ds. \tag{1.205}$$

Substituting for $X(T)$ into this equation gives

$$\left\langle \int_0^T f(t)dW(t) \int_0^T f(s)dW(s) \right\rangle = \int_0^T f(s)^2 ds,$$

which can be captured by the rule

$$\langle dW(t)dW(s) \rangle = \delta(t-s)dt\,ds. \tag{1.206}$$

However, care must be taken with this rule when $\delta(t-s)$ appears inside an integral having t or s as one of its limits. For example, consider the double stochastic integral

$$\int_0^T \left[\int_0^t f(s)dW(s) \right] g(t)dW(t) \equiv \lim_{N \to \infty} \sum_{n=0}^{N-1} \left[\sum_{m=0}^{n-1} f(t_m)dW_m \right] g(t_n)dW_n.$$

We see that there are no terms in the double sum on the right-hand side that have a product of Wiener increments in the same time interval. Thus, taking the expectation of both sides,

$$\left\langle \int_0^T \left[\int_0^t f(s)dW(s) \right] g(t)dW(t) \right\rangle = 0.$$

Hence, we require

$$\int_0^t f(s)\delta(t-s)ds = 0, \quad \int_0^t f(s)\delta(s)ds = f(0). \tag{1.207}$$

Following the previous examples, let us turn to a discretized version of the general SDE for $X(t)$,

$$dX = a(X,t)dt + b(X,t)dW(t), \tag{1.208}$$

which takes the form

$$X_{n+1} - X_n = a(X_n,t_n)\Delta t + b(X_n,t_n)\Delta W_n. \tag{1.209}$$

Iterating this equation starting from a fixed $X(0) = x_0$ yields

$$X_N = x_0 + \sum_{n=0}^{N-1} a(X_n,t_n)\Delta t + \sum_{n=0}^{N-1} b(X_n,t_n)\Delta W_n.$$

The continuum limit then gives the stochastic integral equation

$$X(T) = x_0 + \int_0^T a(X(t),t)dt + \int_0^T b(X(t),t)dW(t), \tag{1.210}$$

with the final term defined as the Ito stochastic integral

$$\int_0^T b(X(t),t)dW(t) = \lim_{N\to\infty} \sum_{n=0}^{N-1} b(X_n,t_n)\Delta W_n. \tag{1.211}$$

The integral equation is not very useful for generating an explicit solution for $X(t)$. However, from the definition of the Ito stochastic integral, it immediately follows that

$$\left\langle \int_0^T b(X(t),t)dW(t) \right\rangle = 0, \tag{1.212}$$

since X_n is a function of previous Wiener increments $\Delta W_{n-1}, \ldots, \Delta W_0$ so it is uncorrelated with ΔW_n. The stochastic difference equation (1.209) is the starting point for developing numerical schemes for solving an SDE. However, if one is interested in carrying out explicit calculations, it is usually more useful to go to the associated Fokker–Planck equation for the probability density. In order to derive the FP equation from the corresponding SDE, we first need to consider the object $(dW)^2$.

In terms of Wiener increments,

$$\int_0^T (dW(t))^2 = \lim_{N\to\infty} \sum_{n=0}^{N-1} (\Delta W_n)^2.$$

Taking the expectation of both sides and using the fact that each ΔW_n is an i.i.d., gives

$$\left\langle \int_0^T (dW(t))^2 \right\rangle = \int_0^T \langle (dW(t))^2 \rangle = \int_0^T dt = T. \qquad (1.213)$$

What about the variance? Using the Gaussian probability density (1.203), it is simple to show that

$$\text{Var}[(\Delta W)^2] = 2(\Delta t)^2 = 2T^2/N^2.$$

Hence,

$$\text{Var}\left[\int_0^T (dW(t))^2\right] = \lim_{N\to\infty} \text{Var}\left[\sum_{n=0}^{N-1} (\Delta W_n)^2\right] = \lim_{N\to\infty} \sum_{n=0}^{N-1} \text{Var}\left[(\Delta W_n)^2\right]$$

$$= \lim_{N\to\infty} \frac{2T^2}{N} = 0.$$

We thus obtain the surprising result that the integral of $(dW)^2$ is deterministic and thus equal to its mean:

$$\int_0^T (dW(t))^2 = T = \int_0^T dt. \qquad (1.214)$$

In other words, we can set $(dW)^2 = dt$, a result known as Ito's rule. Using similar arguments, it can also be shown that $dW^m = 0$ for $m > 2$.

1.7.2 Ito's Formula and the Fokker–Planck Equation

The result $dW(t)^2 = dt$ has important implications for how one carries out a change of variables in stochastic calculus. This is most directly established by considering the SDE for an arbitrary function $f(X(t))$ with $X(t)$ evolving according to (1.208):

$$df(X(t)) = f(X(t) + dX(t)) - f(X(t))$$

$$= f'(X(t))dX(t) + \frac{1}{2}f''(X(t))dX(t)^2 + \dots$$

$$= f'(X(t))[a(X,t)dt + b(X,t)dW(t)] + \frac{1}{2}f''(X(t))b(X,t)^2 dW(t)^2,$$

where all terms of higher order than dt have been dropped. Now using $dW(t)^2 = dt$, we obtain the following SDE for f, which is known as Ito's formula:

$$df(X(t)) = \left[a(X(t),t)f'(X(t)) + \frac{1}{2}b(X,t)^2 f''(X(t))\right] dt + b(X,t)f'(X(t))dW(t).$$

$$(1.215)$$

Hence, changing variables in Ito calculus is not given by ordinary calculus unless f is a constant or a linear function.

We can now use Ito's formula to derive the FP equation for an Ito SDE. First,

$$\frac{\langle df(X(t))\rangle}{dt} = \left\langle a(X(t),t)f'(X(t)) + \frac{1}{2}b(X(t),t)^2 f''(X(t)) \right\rangle$$

$$= \int \left[a(x,t)f'(x) + \frac{1}{2}b(x,t)^2 f''(x) \right] p(x,t)dx,$$

$$= \int f(x)\left[-\frac{\partial}{\partial x}(a(x,t)p(x,t)) + \frac{1}{2}\frac{\partial^2}{\partial x^2}(b(x,t)^2 p(x,t)) \right]dx. \quad (1.216)$$

after integration by parts, where $p(x,t)$ is the probability density of the stochastic process $X(t)$ under the initial condition $X(t_0) = x_0$. However, we also have

$$\frac{\langle df(X(t))\rangle}{dt} = \left\langle \frac{df(X(t))}{dt} \right\rangle$$

$$= \frac{d}{dt}\langle f(X(t),t)\rangle$$

$$= \int f(x)\frac{\partial}{\partial t}p(x,t)dx. \quad (1.217)$$

Comparing (1.216) and (1.217) and using the fact that $f(x)$ is arbitrary, we obtain the Ito version of the FP equation

$$\frac{\partial}{\partial t}p(x,t) = -\frac{\partial}{\partial x}(a(x,t)p(x,t)) + \frac{1}{2}\frac{\partial^2}{\partial x^2}(b(x,t)^2 p(x,t)). \quad (1.218)$$

1.7.3 Multiplicative Noise and Stratonovich Integrals

It turns out that there is more than one way to define a stochastic difference equation driven by an incremental Wiener process and thus more than one way to obtain an SDE in the continuum limit. This issue only arises in the case of multiplicative noise, that is, when the term multiplying $dW(t)$ depends on the state variable $X(t)$. Recall that in the Ito integral (1.211), it is the value of $b(x,t)$ at the start of the nth time step that multiplies ΔW_n, so that there are no contributions of the form $(\Delta W_n)^2$. An alternative definition of a stochastic integral is the Stratonovich integral

$$\oint_0^T b(X(t),t)dW(t) = \lim_{N\to\infty}\sum_{n=0}^{N-1} b\left(\frac{X_{n+1}+X_n}{2},t_n\right)\Delta W_n, \quad (1.219)$$

where we have used $\oint$ to distinguish it from the Ito integral. Now b depends on the value X_{n+1} at the end of the nth time step, which means there will be an extra term involving $(\Delta W_n)^2$. In order to compare the Ito and Stratonovich integrals, suppose that X_n evolves according to the stochastic difference equation (1.209). Thus, in the

continuum limit $X(t)$ is the solution to an Ito SDE. Suppose that we Taylor expand the nth term in the sum defining the Stratonovich integral about the point X_n and set $b_n = b(X_n, t_n)$:

$$b\left(\frac{X_{n+1} + X_n}{2}, t_n\right) = b_n + \frac{\Delta X_n}{2}\frac{\partial b_n}{\partial x} + \frac{1}{2}\left(\frac{\Delta X_n}{2}\right)^2\frac{\partial^2 b_n}{\partial x^2} + \dots$$

Substituting for ΔX_n using (1.209) and dropping terms that are higher order than Δt shows that

$$b\left(\frac{X_{n+1} + X_n}{2}, t_n\right) = b_n + \left(\frac{a_n}{2}\frac{\partial b_n}{\partial x} + \frac{b_n^2}{8}\frac{\partial^2 b_n}{\partial x^2}\right)\Delta t + \left(\frac{b_n}{2}\frac{\partial b_n}{\partial x}\right)\Delta W_n.$$

Applying this result to the sum appearing in the definition of the Stratonovich integral, (1.219), and again dropping higher-order terms in Δt, yields the result

$$\sum_{n=0}^{N-1} b\left(\frac{X_{n+1} + X_n}{2}, t_n\right)\Delta W_n = \sum_{n=0}^{N-1} b_n \Delta W_n + \sum_{n=0}^{N-1}\frac{b_n}{2}\frac{\partial b_n}{\partial x}(\Delta W_n)^2.$$

Finally, taking the continuum limit with $dW(t)^2 = dt$, we have

$$\oint_0^T b(X(t),t)dW(t) = \int_0^T b(X(t),t)dW(t) + \frac{1}{2}\int_0^T \frac{\partial b(X(t),t)}{\partial x}b(X(t),t)dt.$$
$$(1.220)$$

Now suppose that $Y(t)$ is a stochastic process evolving according to the Stratonovich SDE

$$dY = a(Y,t) + b(Y,t)dW(t). \tag{1.221}$$

This means that the integral equation satisfied by $Y(t)$ is based on the Stratonovich integral, that is,

$$Y(t) = y_0 + \int_0^t a(Y(s),s)ds + \oint_0^t b(Y(t),t)dW(t). \tag{1.222}$$

Using (1.220), we can rewrite the solution in terms of an Ito integral according to

$$Y(t) = y_0 + \int_0^t \left[a(Y(s),s) + \frac{1}{2}\frac{\partial b(Y(s),s)}{\partial y}g(Y(s),s)\right]ds + \int_0^t b(Y(s),s)dW(s).$$
$$(1.223)$$

The latter is the solution to an equivalent Ito SDE of the form

$$dY = \left[a(Y(t),t) + \frac{b(Y(t),t)}{2}\frac{\partial b(Y(t),t)}{\partial y}\right]dt + b(Y(t),t)dW(t). \tag{1.224}$$

Finally, given that we know the FP equation corresponding to an Ito SDE, we can immediately write down the FP equation corresponding to the Stratonovich SDE equation (1.221):

$$\frac{\partial}{\partial t}p(y,t) = -\frac{\partial}{\partial y}(a(y,t)p(y,t)) + \frac{1}{2}\frac{\partial}{\partial y}\left(b(y,t)\frac{\partial}{\partial y}[b(y,t)p(y,t)]\right). \tag{1.225}$$